A

THESIS

ON

PHOTOCATALYTIC DEGRADATION OF HAZARDOUS SAFRANIN (O) DYE BY USING SELF SYNTHESIZED TiO_2 NANOPARTICLES

Submitted by

Mr. SOYAB SALIM BAGWAN

Roll No. 213CH1114

In partial fulfilment for the award of the degree of

MASTER OF TECHNOLOGY

in

CHEMICAL ENGINEERING

Under the Supervision of

Dr. ARVIND KUMAR

DEPARTMENT OF CHEMICAL ENGINEERING

NATIONAL INSTITUTE OF TECHNOLOGY ROURKELA

MAY 2015

NATIONAL INSTITUTE OF TECHNOLOGY ROURKELA

CERTIFICATE

This is to certify that **Mr. Soyab Salim Bagwan** has carried out a project work on **"Photocatalytic Degradation of Hazardous Safranin (O) Dye by Using Self Synthesized TiO_2 Nanoparticles"** in partial fulfilment of the requirements for the award of Master of Technology degree in Chemical engineering, Department of Chemical Engineering at National Institute of Technology, Rourkela is an authentic work carried out by him under my supervision and guidance.

Date:

Dr. Arvind Kumar

(Supervisor)

ACKNOWLEDGEMENT

In pursuit of this academic endeavour, I feel that I have been singularly fortunate; inspiration, guidance, direction, co-operation, love and care all came in my way in abundance and it seems almost an impossible task to acknowledge the same in adequate terms. My guide, **Dr. Arvind Kumar** has been an absolute fount of knowledge during the last couple of months and his patience and inherent kindness have helped me acclimatize, especially in the beginning, to a culture that was not similar to that of mine. I have always enjoyed my conversations with him and will carry on with me several valuable lessons that I have learned. The open-mindedness and freedom of thought encouraged by him was critical as I learned a lot from this atmosphere while his cheerfulness and his encouragement have bolstered me numerous times.

I would like to thank the entire faculty of chemical engineering department as whatever knowledge I earned from them was very useful in this work. I also want to acknowledge all my friends and seniors (Ph.D. scholars) in Chemical Engineering Department as they helped me a lot during the work.

Date:

Mr. Soyab Bagwan

Roll No. 213CH1114

ABSTRACT

The textile industries generates extremely high amount of colour waste water, which are mainly poisons. A traditional biological treatment process is not helpful in treating the dye effluent because of low biodegradability of dyes. The presence of safranin (O) dye causes distinct acute impact on health therefore the removal of this dye from aqueous solution is highly desirable. The aim of this study was to assess the efficiency of photo-degradation of safanin (O) dye with application of nanoparticles of TiO_2 as a photocatalyst. For this purpose nanoparticles of TiO_2 were synthesized by a very simple sol-gel method with absence of additives and hydrolysing agents. The synthesized nanoparticles of TiO_2 were characterized by FTIR, XRD, SEM, BET and UV-vis spectroscopy. It was found that change in polymorphic phase occurs as temperature changes from 600 to 800 ^{0}C and also the crystallinity of TiO_2 increases with annealing temperature. The application of prepared TiO_2 nanoparticles for photocatalytic degradation of safranin (O) dye from aqueous solution was explored. It was determined that anatase phase TiO_2 shown highest photo-degradability of safranin (O) dye. The blank tests investigated for light irradiated to safranin (O) dye solution without TiO_2 catalyst and for the suspension carrying TiO_2 and safranin (O) dye in the dark that revealed both the photocatalyst and light energy were required for the photo-degradation of safranin (O) dye. The effect of several factors such as catalyst dose, initial concentration, pH of solution and temperature, was studied on the photocatalytic degradation of safranin (O) dye and optimized it. Results indicated that photo-degradation of safranin (O) dye increases at higher alkaline pH. The photo-degradation rate was strongly influenced by activation of TiO_2 photocatalyst with photon and production of hydroxyl radicals' hence suggested optimum catalyst dose and initial concentration of dye for photo-degradation process.

KEYWORDS: TiO_2 nanoparticles, Sol-gel synthesis, Safranin (O) dye, Photocatalysis.

CONTENTS

LIST OF FIGURES

LIST OF TABLES

NOMENCLATURE

BET = Brunauer-Emmett-Teller

CB = Conduction band

C_s = concentration of safranin (O) dye (in ppm) after a time t in (mins),

C_{s0} = concentration of safranin (O) dye (in ppm) at time t=0 min,

CVD = Chemical vapour deposition

D = Average crystallite size in ^{0}A

FTIR = Fourier transform infrared

FWHM = Full width half maximal

GaAs = Gallium arsenide

hυ = Photon energy

k = the pseudo fiest order rate constant of photo-degradation process,

M = metal

PVD = Physical vapour deposition

R = Alkyl group

r = Water to alkoxide ratio

SEM = secondary electron microscope

SPD = spray pyrolysis deposition

t = time in mins.

TiO_2-110 = TiO_2 dried at 110 ^{0}C

TiO_2-400 = TiO_2 calcinated at 400 ^{0}C

TiO_2-600 = TiO_2 calcinated at 600 ^{0}C

TiO_2-800 = TiO_2 calcinated at 800 ^{0}C

TTIP = Tittanium tetra isopropoxide

UV = Ultra violet

VB = Valance band

XRD = X ray diffraction

β = Line width at half maximum intensity

ε = Dielectric constant

θ = Braggs angle

λ = Wavelength of

K = Shape f.actore (0.9 is used)

Chapter 1

INTRODUCTION

1. INTRODUCTION

ABSTRACT: This section includes basic understanding of dyes, safranin (O) dye and TiO_2 nanoparticles as well as the impact of dyes especially safranin (O) dye on the environment and aquatic life has discussed. Various treatments to remove the dye from waste stream were discussed. Also properties that existed in TiO_2 nanoparticles and its applications were explained. Process of photocatalysis using TiO_2 as a photocatalyst was summarized.

BACKGROUND STUDY: There is emerging public concern over the contamination of wastewater by dyes. Therefore, a major focus of research has been on the removal of dyes and pigments from wastewater. This is because of the fact that existence of dyes and pigments in water is highly unwanted, even at very low concentrations, [1]. Total annual manufacturing of dyes in the world is more than 7×10^5 tons and about 2% of dyes produced annually are released in effluent from manufacturing operations [2]. India has become a notable manufacturer of dyes and pigments during the past 35 years, to satisfy the requirement of not only the textile industries but also of other industries such as printing inks, plastics, rubber, paints, paper, art and craft, cosmetics, leather, food and drug [3]. Release of dye effluents into the environment is presently one of the world's crucial environmental problems for both esthetic reasons and toxicological.

Safranin (O) is one of the most frequently used azine dye, which is among the oldest well known synthetic dyes. Safranin (O) is a water-soluble reddish brown powder, which is mainly used to dye silk, wool, tannin, cotton, bast fibers, silk, leather and paper. Also it has wide application in textile, trace, biological laboratory purpose [4]. The presence of safranin (O) causes distinct acute impact on health like irritation to mouth, tongue, throat, lips and pain in stomach which may lead to vomiting, nausea and diarrhea [5]. Thus, the `withdrawal of safranin (O) dye from the aqueous solution is highly desirable. Dye containing effluents are commonly processed by physical or chemical processes. The conventional methods for treatment of dye containing wastewater are oxidation, degradation of biological compound, flocculation, coagulation and physical separation have been extensively explored to remove various dyes from wastewaters [6–8].

The textile industries generates extremely high amount of color wastewater, which are mainly poisonous. A mandatory criterion for these dyes in their application is that they should be exceptionally stable in sun light and during washing. Also they should oppose the

effect of microbial attack. So that, they aren't easily degrade and by commonly used chemical effluent treatment systems they are not readily removed from wastewater [9]. A traditional biological treatment process is not helpful in treating the dye effluent because of low biodegradability of dyes [10]. A broad range of traditional physical and chemical processes like oxidation, irradiation, electro-flotation, flocculation, precipitation, membrane filtration, ion exchange and electro-kinetic coagulation have been examined immensely for withdrawing dyes from aquatic bodies [11, 12]. However, a broad range of wastewater containing dyes cannot be effectively treated by these processes and also they are costly [13]. Two convenient technologies for removal of dye are adsorption and oxidation. Out of these two, the possibly best technology to totally eliminate organic carbons is oxidation methods

The supremacy of photo-degradation process by semiconductors in dye effluent treatment is because of its advantages over the conventional methods, such as quick oxidation, oxidation of pollutants and no formation of polycyclic products. It is a powerful and quick method for the withdrawal of pollutants from effluent [14, 15].

Titanium dioxide (TiO_2) is a widely used multifunctional material due to its physical & chemical properties, excellent stability as well as its non-toxicity, great accessibility and moderate cost. Commercially they can be found in coatings, paints, pigments and sunscreens [16, 17]. TiO_2 quickly attracted numerous research interests because of its highly active photocatalytic activity, like its ability to degrade chemical compounds as well as superhydrophilic, antibacterial properties, and energy-related applications. The UV photon is capable to excite (activate) the photocatalyst, which results in the excitation of an electron from the valence band (VB) to the conduction band (CB). Although, one of the major problem which decrease the effectiveness of photocatalysis process is recombination of photo-generated electrons and hole pairs. The excellent surface activity and appropriate electronic band structure favors TiO_2 with very promising potentials in hydrogen production, photovoltaic, photocatalyst, lithium-ion batteries and fuel cells [18]. Fujishima and Honda in 1972, found the phenomenon of splitting of water on a TiO_2 photocatalyst under UV light. After this, a plenty of efforts have been committed to the study of TiO_2 material, which has developed large number of positive applications in various areas from photovoltaic and photocatalysis to various sensors. These applications can approximately categorized into two categories, 'environmental' and 'energy', most of them depend on the properties of the TiO_2 material, modifications of the TiO_2 material host (e.g., with organic dyes and inorganic dyes) and also on the interactions of TiO_2 materials with the environment [19]. In the past decades,

an enormous development in research activities has been seen in nanotechnology and nanoscience. A new physical and chemical property emerges when the size of the material reduced smaller and smaller. TiO_2 bears huge faith in helping ease the energy crisis through efficiently utilization of solar energy based on water-splitting devices and photovoltaic. In recent years, as continue research work have been made in the preparation, modification, and applications of TiO_2 nanoparticles. TiO_2-based nanoparticles recently showed the highest effectiveness in photocatalytic water splitting by narrowing bandgap energy, to permit visible light photo activities. Nevertheless, although TiO_2 hold such potentials, its relatively unsatisfactory wide bandgap (~3.2 eV) and charge transport property are two important limitations for its present-day utilization in energy harvesting (or storage) and catalysis [20].

In fact, on nanoscale morphologies of TiO_2 most of its applications were based, especially the nanoparticles form. In the nanoscale, Because of the emergence of the quantum confinement effects, the transport behaviours of electron and hole could be varied, and the electronic band structure could be shifted. The huge surface-to-volume ratio of nanomaterial can remarkably increases the reaction sites at surface and can even adjust the surface atoms catalytic activity. In the nanoscale structures particular high energy surfaces should also become stable and enhance their catalytic properties. Therefore, on the establishment of appropriate nano-size structures with well arranged composition, geometry, integration, and crystallography can further enhanced the performance of TiO_2 semiconductor based systems and devices[21].

In obtaining the final TiO_2 material properties, controlling the shape, structure and size of the colloidal precursor are very important factors. TiO_2 powders have been acquired either by precipitation from solutions of titanium salts or alkoxides or directly from titanium-bearing minerals. The most ordinary methodologies were relied on the hydrolysis of acidic solutions of Ti (1V) salts [6]. To prepare finely divided titania powders with high purity, hydrolysis reactions of titanium alkoxides and the gas-phase oxidation reactions of $TiCl_4$ were used. However, these titania powders have usually lacked in the properties like constant (uniform) shape and size, also unagglomerated state required for quantitative studies of colloidal phenomena [22]. Recently, through controlled nucleation and growth processes in dilute Ti (IV) solutions, lots of methodologies were published for preparing titania nanoparticles. Some of them are the sol-gel method and hydrothermal method, which are having advantage of low reaction temperature. It has been revealed that the initial nanostructure of titanium dioxide precursors sinthesized by hydrolyzing titanium alkoxide, strongly affects the

characteristics of the final powder and crystallization behaviour [23]. In this report, we have tried to prepare anatase and rutile TiO_2 by relatively simple sol-gel method and an attempt is made to look at the degradation of the safranin (O) dye in aqueous solution in presence of UV light by using synthesized TiO_2 nanoparticles.

1.1. OBJECTIVE OF WORK

The specific objective of these studies to do investigation for photocatalytic degradation of basic dye safranin (O) from wastewater using nanoscale self prepared TiO_2 Photocatalyst.

- Preparation of nanoparticles of TiO_2 by sol-gel method from TTIP as Ti source and isopropyl alcohol as solvent.
- Synthesis of TiO_2 nanoparticles without using any additives and hydrolysing agent.
- Characterization of prepared TiO_2 nanoparticles to determining various properties, by using XRD, FTIR, UV-vis spectroscopy and SEM etc.
- Investigate the potential of synthesized TiO_2 nanoparticles as a photocatalyst under UV radiation for oxidation of safranin (O) dye in aqueous solution.
- Study of different operational parameters such as catalyst loading, initial dye concentration, pH and temperature on the rate of photo-degradation of the safranin (O) dye.
- Study the kinetics of the photo-degradation of safranin (O) dye in presence TiO_2 photocatalyst and UV radiation.

Chapter 2

LITERATURE REVIEW

2. LITERATURE REVIEW

ABSTRACT: Various literatures have been studied on TiO_2 nanoparticles and represented here in this section. The brief discussion on various crystal structures, synthesis procedure and reaction mechanism of TiO_2 nanoparticles were also given. This content contains the details of photocatalysis process and factors affecting photocatalysis such as catalyst dosage, pollutant concentration, pH, temperature etc.

2.1. PROPERTIES OF TITANIUM DIOXIDE

Table 1- Properties of Titanium dioxide (TiO_2) [22]

Properties of Titanium dioxide (TiO_2)	
Molecular Formula	*TiO_2*
Molecular Weight	*79.866 g/mol*
Density	*4.24 g/cm3 (Rutile)* *3.77 g/cm3 (Anatase)*
Melting Point	*1844 °C*
Boiling point	*2973 °C*
Refractive index (nD)	*2.489 (Anatase)* *2.584 (Brookite)* *2.608 (Rutile)*
Appearance	*White solid*
Solubility	*Insoluble in water*
Odour	*Odourless*

2.2. CRYSTAL STRUCTURE OF TiO_2

Banfield J. F. et.al., (1992), [23] studied the various crystal structure of TiO_2. TiO_2 normally exhibits four various types of polymorphic phases, which are anatase, rutile, TiO_2(B), and brookite. Also there are several metastable polymorphic phases, such as TiO_2 (H) (hollandite), TiO_2 II (columbite), TiO_2 III (baddeleyite) and TiO_2(R) (ramsdellite) have been synthesized synthetically. Various polymorphic phases have different types of properties and therefore needs different types of conditions to obtain desired polymorphic phases and provide different type of performance.

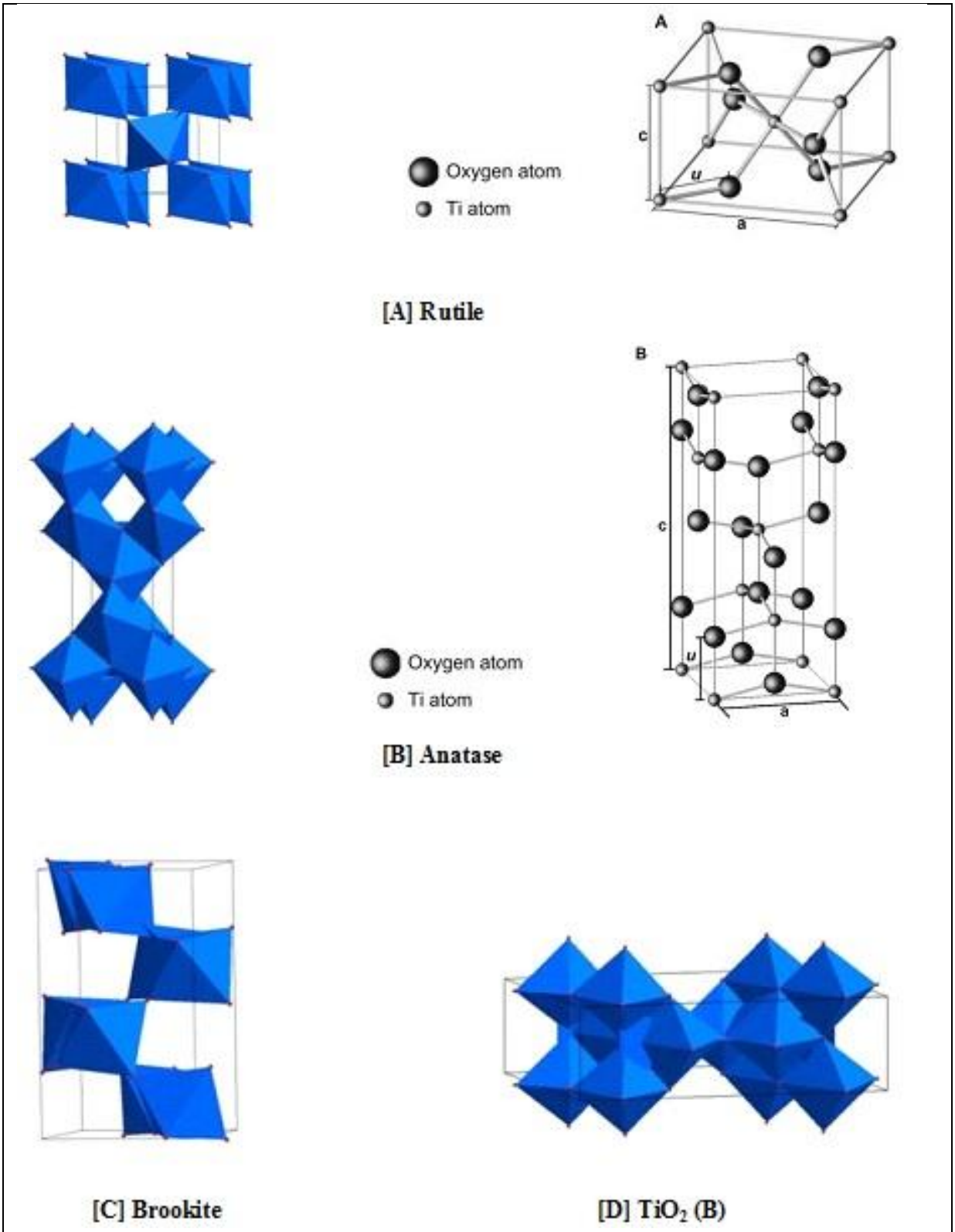

Figure 1: Crystal structure of the four common TiO_2 phases. [23]

Generally, anatase, brookite, and TiO_2 (B) are metastable phases, while rutile is the most stable phase and these anatase, brookite, and TiO_2 (B) phases can transform into rutile phase under high temperature. This phase stability relationship also exists in TiO_2 nanomaterial formations. A polymorphic phase which is commonly obtained in nanomaterials is anatase phase. Anatase phase always found in low-temperature vapor deposition or solution-based systems. Annealing or high temperature deposition would generally yield rutile phase nanostructures of TiO_2. TiO_2 (B) and Brookite polymorphic phases are typically obtained from solution-based growth systems and also less common in nature. Using particular types of precursors and under restrict conditions these other types of metastable phases can be synthesized. Thus we will not consider these metastable phases in this project because they rarely obtained as a stable phase in nanomaterial. Figure 1 shows the schematic structure of crystal of four different TiO_2 phases by using the fundamental building block as Ti−O octahedrons.

These four anatase, rutile, brookite, and TiO_2 (B) polymorphic phases have different nanostructures which always exhibit different growth behaviors and preferred morphologies as well as shows different symmetry. Rutile phase TiO_2 material shows a tetragonal structure with (Figure 1 [A]). The thermodynamically equilibrium morphology of rutile phase TiO_2 is a trunked octahedron due to its two surface families {011} and {100} have the lowest energy. Rutile phase is one that mostly observed morphology from synthetic TiO_2 powders. The anatase phase also shows tetragonal crystal structure but has a significantly longer c-axis compared to the a-axis; Figure 1 [B]). Anatase phase TiO_2 shows trunked octahedron morphology in its nanostructures same as the rutile phase with same lowest energy surfaces.Brookite shows orthorhombic crystal structure and has a large unit cell consisting of 8 TiO_2 groups (Figure 1 [C]). This large unit cell also present in TiO_2 (B) with comparatively more open crystal structure than other polymorphic phases (Figure 1 [D]). TiO_2 (B) is monoclinic having a particularly long a-axis (1.216 nm). Whereas, both brookite and TiO_2(B) phases are less regularly obtained in synthetic TiO_2 nanostructures.

Gong X. Q. et al., (2006), [24] concluded that the first step toward reasonable experimental design for preparing TiO_2 nanoparticles with well specified dimension, shape, crystallinity and phase, which is the primary importance for accomplishing desired functionality and performance is understanding the crystal structure.

2.3. SYNTHESIS PROCEDURE OF TiO_2

The TiO_2 can be prepared in the form of different powder, thin films, and crystals forms by two well defined routes, namely by **O. Carp et al., (2004),** [25],

1. Solution route synthesis

2. Gas phase synthesis

2.3.1. SOLUTION ROUTE SYNTHESIS

This route is usually used to synthesize thin films of TiO_2 because of it is convenient and easy. Also it gives a control over homogeneity and stoichiometry, the synthesis of composite materials as well as formation of complex shapes. The demerits of this route lie in its high cost, large processing time as well as presence of impurities, such as carbon.

Some commonly used solution route synthesis methods are given below,

1. Sol-gel methods

2. Sol-Method

3. Hydrothermal methods

4. Solvothermal methods

5. Precipitation methods

2.3.2. GAS PHASE SYNTHESIS

The specialty of this route is forming coatings to alter different properties, such as the electrical, thermal, mechanical, optical, wear resistance and corrosion resistance properties of various substrates. They can be also be used to synthesize composite materials by the process of infiltration. The commonly used gas phase methods are,

1. Chemical vapour deposition (CVD)

2. Physical vapour deposition (PVD)

3. Spray pyrolysis deposition (SPD)

2.4. SOL-GEL SYNTHESIS

Larry L. H. et al., (1990), [26] concluded that out of these mentioned methods, sol–gel method is one of the most widely used for synthesizing TiO_2 nanaoparticles, due to various advantages, such as high homogeneity of particles, low processing temperature, synthesis conditions, stability and versatility of processing. In this sol-gel method, we have to mix to different solutions and these two solutions are generally called as precursor and hydrolysis solution. In sol-gel method hydrolysis solution is added dropwise to the precursor solution at room temperature under vigorous stirring to control the hydrolysis rate and therefore the particle size of TiO_2. It is commonly proclaimed that the most delightful characteristic of sol–gel processing is the possibility of customizing unique materials, mainly by polymerization of a metalorganic compounds to obtain a polymeric gel. An important thing is that, designing the proper monomer that will polymerize to obtain M-O-M structures (where M is the metal and O is the oxygen atom). Metal alkoxides, M(OR)*n*, (where M is the metal and R is an alkyl radical), fulfil these needs. Most reports on sol–gel method for preparation of TiO_2 nanoparticles involved titanium alkoxide (titanium isopropoxide [TTIP], titanium butoxide, titanium ethylhexoxide and tetra-n-butyl titanate) as Ti source material. Few researchers used $TiCl_4$ as the Ti precursor solution.

Brinker C. J. et al., (1999), [27] was focused the attention on one of the most commonly used precursors, metal alkoxides, that have an organic ligands attached to a metal or metalloid atom. Their popularity arises out of their high reactivity with water. The term ceramic is an 'umbrella' that covers all materials that are metal oxides, nitrides or carbides, both non-crystalline and crystalline. A sol can be defined as a colloidal suspension of solid particles (1-1000nm) in a liquid, and that is dominated by short range forces such as Van der Waals forces and surface charges. While, A gel incorporates two phases having colloidal dimensions; a continuous liquid phase enclosed by a continuous solid skeleton. A gel is grown from, either, mechanical mixing of discrete colloidal particles at a pH that prevents precipitation, or, from an interconnected 3-D network formed during the hydrolysis and poly-condensation of the precursor.

Jagdale T. C. et al., (2008), [28] described the several routes that can be followed to obtain sol-gel monoliths are represented in Figure 2. The resultant product obtained when a gel is dried under ambient conditions by evaporation is called a xerogel. The volumes of these xerogels are usually 5 to 10 times less than the volume of original gel. However, when the gel is dried in an autoclave, the resultant product is known as an aerogel.

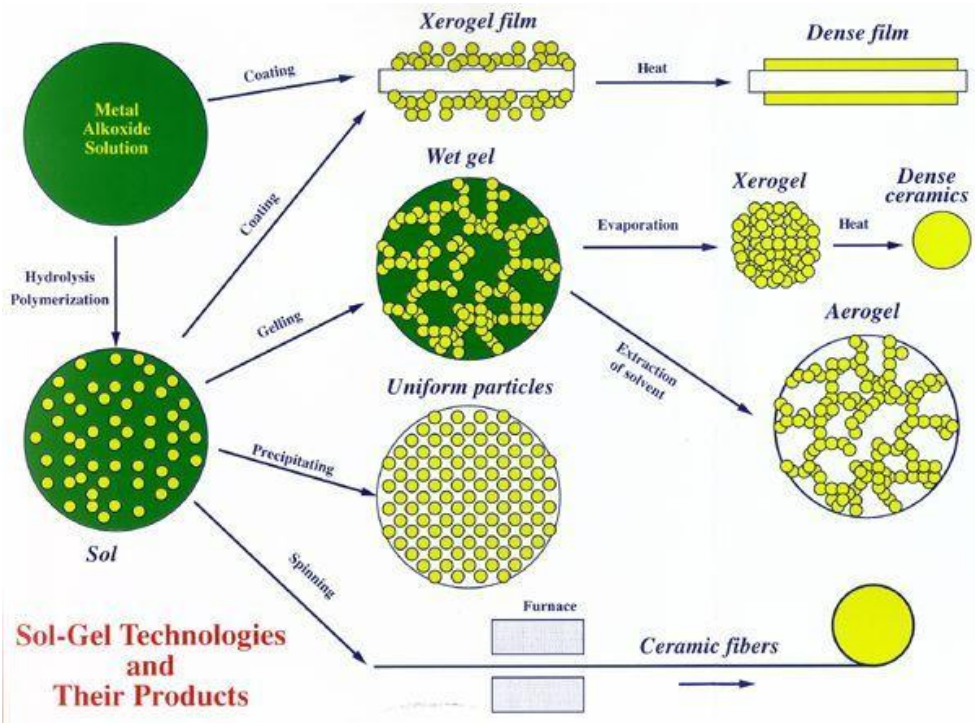

Figure 2 Sol-gel process [29].

An aerogel has almost the same volume as the volume of original gel, due to the lack of capillary pressure while drying.

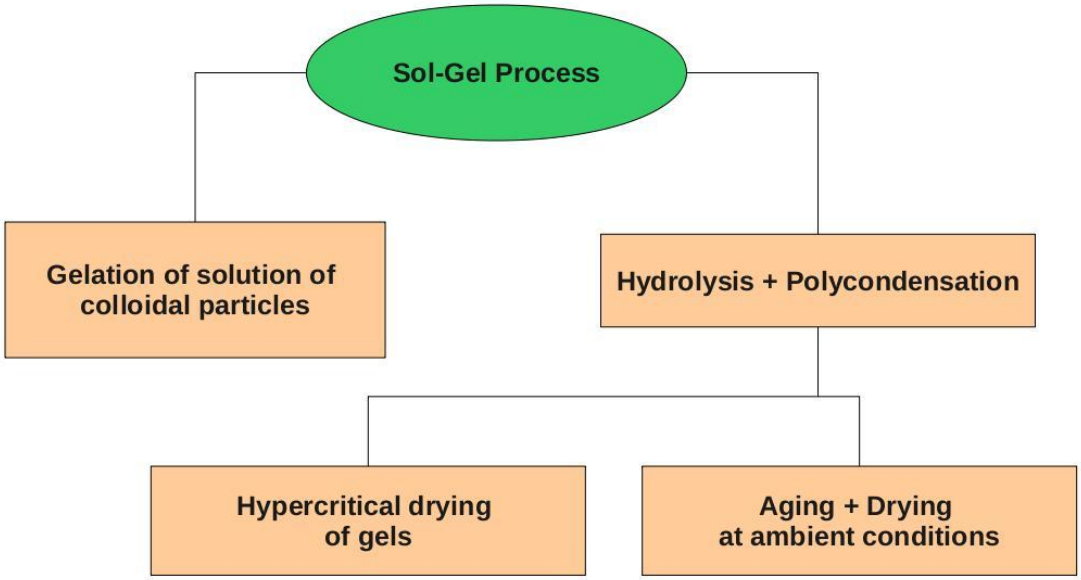

Figure 3 Sol-gel routes to obtain monoliths adapted from [28].

As shown in Figure 3, the structure of the gel based on the gelation route. For gels formed by the hydrolysis and condensation route, the structure depends heavily on the kinetics of these reactions. The processes that succeed ageing, drying, stabilization, and densification steps rely on the gel structure.

2.4.1. REACTION MECHANISM

Lee J. H. et al., (2005), [29] shown the sol-gel method is depends on inorganic polymerization reactions. This involves various steps such as hydrolysis, poly-condensation, drying of material and then thermal decomposition (calcination). In the first step, hydrolysis of the precursors of the metal or non-metal alkoxides carried out with either water or alcohols.

$$Ti(OR)_4 + 4H_2O \longrightarrow Ti(OH)_4 + 4ROH \text{ (hydrolysis)}$$

Where R = alkyl group

Zhang H. et al., (2002), [30] and **Oskam G. et al., (2003),** [31] explained in addition to water and alcohol, also a base or an acid helps in the hydrolysis of the precursor solution. Generally this process begins and continues with the hydrolysis step of titanium (IV) alkoxide by an acid-catalyzed hydrolysis and followed by condensation. The generation and growth of Ti-O-Ti chains is recommended with low water content, low rates of hydrolysis and an excess amount of titanium alkoxide solution in the reaction media. However, close packing of three dimensional polymeric skeletons are obtained by the establishment of Ti-O-Ti chains. The generation of titanium hydroxide (Ti-$(OH)_4$) is recommended by high rates of hydrolysis for a medium amount of water.

Behnajady et al., (2011), [32] represented the presence of a large amount of Ti-OH and insufficient establishment of three-dimensional polymeric skeletons lead to loosely packed first-order particles. In the existence of a large excess of water, the polymeric Ti-O-Ti chains are developed. And via a three-dimensionally developed gel skeleton a closely packed first order particles are yielded.

$$Ti(OH)_4 \longrightarrow TiO_2 + 2H_2O \text{ (condensation)}$$

Calcinations at higher temperature are required to decomposition of the organic precursor. The flow chart of sol-gel method for the preparation of TiO_2 nanoparticles has been shown in Fig. 5.

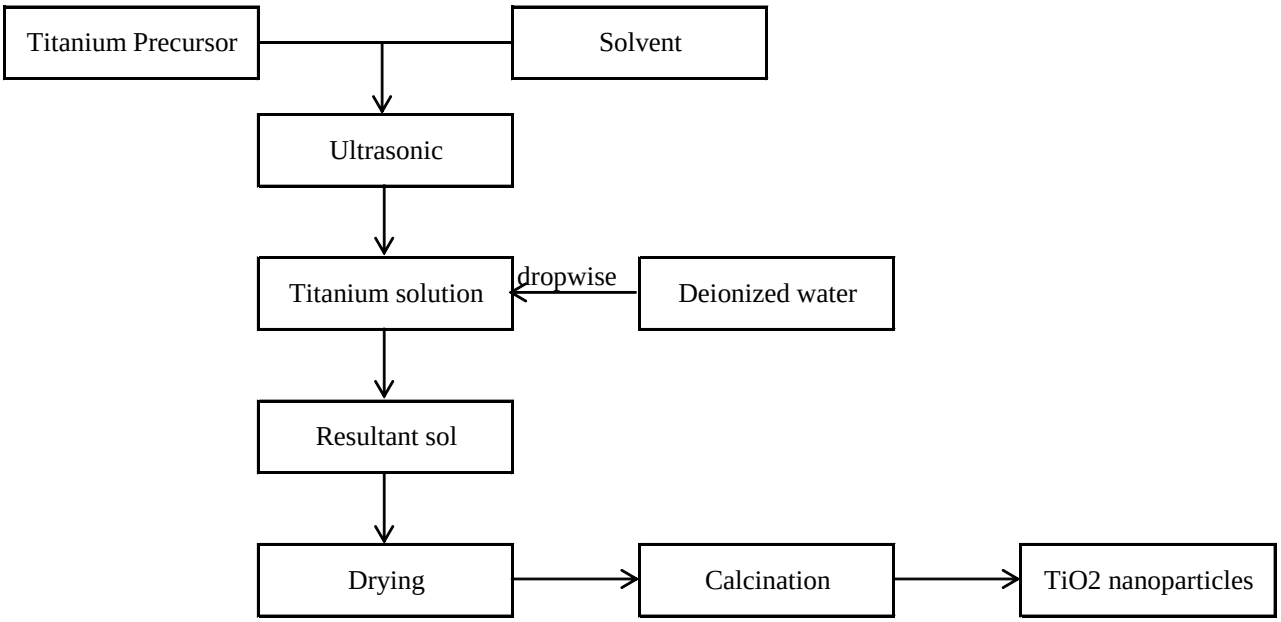

Figure 4 Scheme of preparation of nanoparticles sol-gel method. [32]

Burda C. et al., (2005), [33] concluded the size of sol particles depends on the pollution composition, pH and temperature. By controlling these factors, one can tune the size of the particles.

Tumma H. et al., (2009), [34] shown that from titanium tetra isopropoxide (TTIP), triethanolamine, and mild acids like acetic acid are used generally to prepare phase pure anatase nanoparticles. A fraction of the product normally comprises the brookite phase nanoparticles, when stronger acids are used. The preparation of brookite phase nanoparticles has been given by thermolysis of TiCl4 in aqueous solution of HCl. The reaction product composition was obtained to be strongly dependent on the concentration ratio of Ti:Cl (approx near about 17–35). Phase pure rutile phase TiO_2 nanoparticles have been synthesized from titanium tetra isopropoxide (TTIP) in nitric acid at pH = 0.5, or from $TiCl_4$ or $TiCl_3$ in HCl solution.

Loryuenyong V. et al., (2011), [35] studied that the preparation of nanoparticles TiO_2 by a sol-gel method, by using titanium tetra isopropoxide as a precursor and ethanol or 2-propanol (isopropyl alcohol) as an alcoholic solvent. The prepard mesoporous TiO_2 was annealed at about 300–800°C. It was explained that the anatase to rutile phase transformation, crystallite growth, and pore collapsing occurred with an increase in calcinations temperature. To inhibit the anatase to rutile transformation a solvent isopropyl alcohol was used, and this transformation inhibited by the controlling the rate of hydrolysis. An improvement in the

degradation of methylene blue under UV light was observed by the TiO_2 photocatalyst containing predominantly of anatase crystallites. Also an improved photocatalytic activity was obtained with 2-propanol solvent through the thermal stability of anatase phase as compared to ethanol.

2.5. HETROGENOUS PHOTOCATALYSIS

The late twentieth century saw the arising of a novel advanced oxidation process (AOP) called heterogeneous photocatalysis, now holding over a thousand research articles published annually. This process has since been utilized in a large variety of reactions, specially, dehydrogenation, water purification treatment and hydrogen transfer. An apt definition of a photocatalyst is quoted here, from an article by **Jean-Marie Herrmann** [36], \Photocatalysis is based on the double aptitude of the photocatalyst (essentially titania) to simultaneously adsorb both reactants and to absorb efficient photons ($h \geq E_g$)".

As reported by **Herrmann et al., (2010),** [36] the phenomenon may be divided into 5 steps that take place sequentially:

1. Transfer of the reactants from the fluid phase to the surface,
2. Adsorption of the reactants on the surface,
3. At this point, activation of the reaction in the adsorbed phase by the photons (UV or visible irradiation)on the surface,
4. Desorption of the products,
5. Removal of the products from the interface region.

To enhancing the external quantum efficiency of steady state photocatalytic processes, which is the percentage of the photons generating an electron-hole pair, it is most important to focus on increasing either the lifetime of charge-carrier or the interfacial electron transfer.

There is some dispute in the scientific community, over the role of VB holes; some suggest that they are directly responsible (before trapping) for the degradation of organic compounds, while others propose that degradation occurs indirectly by trapped holes at the surface (surface bound hydroxyl ion). It is hard to differentiate between the two mechanisms as both of them in oxygenated aqueous solutions produces similar products.

It is reported by **S. Parra et al., (2002),** [37] that for the photo degradation process to occur, the target molecule (usually pollutant) has to be adsorbed on the surface of semiconductor. On the other hand, there are some investigations that report that while adsorption of the target molecule will enhance the rate of the degradation process, it is not a prerequisite. This is because of the OH radicals can diffuse into the fluid phase and can react with the target molecule. In conclusion, while there appears to be some contradiction in the studies obtained regarding the requirement of adsorption of the target molecule, it does seem to be clear that the degradation rate increases when there is adsorption, and therefore is a vital factor in the photocatalytic process.

2.6. TITANIUM DIOXIDE AS A PHOTOCATALYST

For an ideal photocatalyst, **O. Carp et al.** [25] state the following characteristics:

1. Biologically and chemically inert,
2. Photocatalytically stable,
3. Easy to prepare and to use,
4. Effectively activated by sunlight,
5. Able to effectively catalyze reactions,
6. Cheap
7. Non-toxic to the environment and humans.

The semiconductor that comes closest that having the above mentioned criteria is TiO_2. The main disadvantage in using TiO_2 is its lack of absorption in the visible region of the electromagnetic spectrum.

Y. Kubota et al., (2001), [38] the indiscriminate, high-potential (2.80V) oxidizing agents (holes and OH radicals) generated when TiO_2 is exposed to the light are widely used to degrade environmental pollutants likewise organics, fungi, viruses and bacteria into harmless products such as H_2O, CO_2 and into other inorganic harmless molecules. This indiscriminate response of the TiO_2 catalyst has to be controlled in certain applications to prevent severe damage in these types of cases, as in paints to prevent chalking due to loss of pigments.

Shan Cong et al., (2011), [39] studied that from a point of view of thermodynamics, anatase phases and rutile phase are both capable of initializing photocatalytic oxidation because of the similarity in their valence band. But despite this, studies show that the anatase form has been identified as the more efficient photocatalyst out of these two forms of crystal. A possible explanation could be due to the lifetime of the charge carriers which has been shown to be longer for anatase when compared to that of rutile. Other studies show that a mixture of anatase and rutile phases to be a better photocatalyst than lone anatase phase. This has been described by the result of a possible synergetic effect due to the combination of the two phases. In a study by **Kurkin et al., (1990),** [40] the photocatalytic degradation of acetone in the gaseous phase increased with the increase in calcination temperature attaining a maximum photocatalytic activity at 450 ^{0}C calcinations temperature. This could be due to the increase in the number of charge carriers at the crystallite surface as a result of improved crystallinity. However, after 450 ^{0}C calcination temperature, there was a decrease in activity which is possibly due to the growth in crystallite size leading to a loss in specific surface area. The difference in efficiency between the two phases may be attributed to several parameters, such as the charge carrier mobility in the matrix of the material, crystallite, specific surface area size and absorption of the photons which is affected by crystallite size and material texture.

Besides its photocatalysis importance, TiO_2 is used in several other applications, such as gas sensors (electrical conductivity varies with the ambient gas composition), biomaterials (haemocompatible with the human body). Due to high dielectric constant ($\varepsilon > 100$) of rutile phase, it is used as a dielectric material. The anatase phase is reported to be preferred over the rutile phase in solar cells, as it is lower temperature phase, has lower density, low dielectric constant and higher electron mobility.

2.7. SAFRANIN (O) DYE

It is widely used in textile industries and for biological purpose. It is generally used to dye wool, tannin mordant cotton and silk. Out of the different dyes presently available, basic dyes are among the brightest class of soluble dyes used by textile industries. Basic dyes are also known as cationic dyes. It is stain which is positively charged (cationic) which can react with material which is negatively charged (anionic). The IUPAC name of Safranin (O) dye is 3,7-Diamino-2,8-dimethyl-5-phenylphenazin-5-lum chloride.

Safranin (O) (known as Basic Red 2) is a typical example of an organic dye that belongs to Quinone-Imine class.The chemical structure of dye shown below,

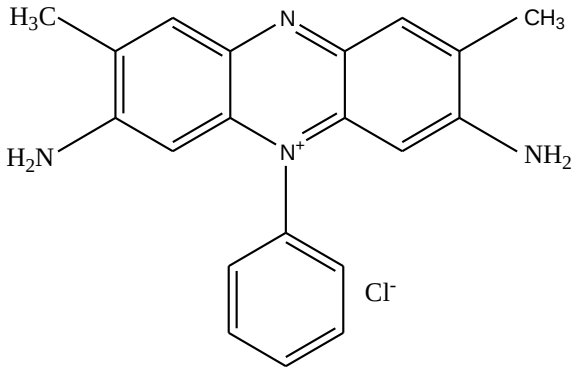

Safranin (Basic Red 2)

In addition to its vast application in dye industries, Safranin is also used as a biological staining in number of biomedical research laboratories and these biological stains are well known to be toxic to human and animals.

Table 2 Molecular Properties of Safanin (O) dye

Properties	***Safranin (O)***
C.I.	*50,240*
Common Name	*Basic Red 2*
Molecular Formula	$C_{20}H_{19}N_4Cl$
Molecular weight	*350.85 g/mol*
Nature	*Powder*
Color	*Redish*
Valance	*+1*
λ_{max}	*520 nm*

Chapter 3

EXPERIMENTAL STUDY

3. EXPERIMENTAL STUDY

ABSTRACT: In this section we discussed various chemical used to prepare TiO_2 nanoparticles as well as instrument used for experiment and analysis. Also we explained the experimental setup especially prepared to carry out the experiments and synthesis procedure for synthesis of TiO_2 nanoparticles.

3.1. CHEMICALS

Titanium (IV) isopropoxide (AcrosOrganics, purity98+%) and Isopropyl alcohol (Merck, 99.5%) used were laboratory-grade chemicals; water from a MilliQ system was used.

3.2. INSTRUMENTS USED

A number of instruments were used throughout the project work to make easy and rapid analysis.

Table 3 List of instruments used for synthesis and analysis

Name of Instrument	***Company Name and Model Name***
XRD	*Ultima IV Multipurpose XRD system*
FTIR	*Thermofisher, Nicolet is10*
SEM	*Jeol, JSM-6480LV*
UV- Visible Spectrophotometer	*Shimadzu, UVSPECTROPHOTOMETER*
BET	*Quantachrome Instruments*
Magnetic Stirrer	*Remi Elektronik Ltd., REMI 2MLH*
pH Meter	*Systronics, µpH system 360*
Weight Balance	*Denvar Instrument, SI-234*
Mercury Lamp	*Bajaj, 125W HPMV (220-250 V)*

3.2.1. X-RAY DIFFRACTION SYSTEM

X-Ray Diffraction analysis instrument is very important and useful machine to characterize various materials, to get the information of determination of lattice parameter and strain as well as for analysis of phase (such as crystalline phase, non-crystalline phase, elemental phase, inter-mettalic phase) and orientation.

The XRD instrument having model name Ultima IV Multipurpose XRD system was used to characterize the TiO_2 samples synthesized by sol-gel method and calcinated at different temperatures. The scanning range of $10\text{-}80^0$ with scanning speed of 5^0/min and voltage of acceleration was 30 KV. The X-pert high score software was used, to analyze the peaks and to identify the various types of phases.

3.2.2. FOURIER TRANSFORM INFRARED (FTIR) SPECTROSCOPY

Fourier Transform Infrared (known as FTIR) spectroscopy used to identification of polymeric, organic and inorganic (in some cases) materials. It uses the infrared radiation to scan the sample and to observe the properties (chemical). These infrared (IR) radiations are allowed to pass through a testing sample. The sample absorbed some amount of IR radiation and some IR radiation transmitted through the sample. In FTIR spectroscopy system, this absorption or transmission (IR radiation) phenomena used to create the absorbance spectra which shows the unique (like fingerprint) chemical bond as well as molecular structure of the sample. The absorbance spectrum shows the various absorbance peaks and these peaks on the spectrum represent functional groups (e.g. alkanes, alkyl, alcohol, keton etc). The absorption of IR radiation at different wavelength indicates different types of bonds and therefore different functional groups. The analytical spectrum of unknown sample is then compared with catalogued of known material spectra, to identify the components.

In the present work, we used 'Nicolet is10, Thermofisher' model of Fourier Transform Infrared spectroscopy to measure the absorbance spectra of IR radiation. The samples to be analyzed were prepared for FTIR analysis by KBr method. In this KBr method, the powdered TiO_2 nanoparticles and KBr mixture were used as sample to be measure.

3.2.3. SECONADARY ELECTRON MICROSCOPE (SEM)

The scanning electron microscope (SEM) which is a type of electron microscope that uses a high energy electrons beam directed towards sample material. In SEM, the electrons generated by the hot filament get accelerated by electric and magnetic fields. These accelerated electrons by interacting with sample material produce the signals and these signals contains the information of surface topography, composition and various other properties like electrical conductivity. Primarily the SEM is used to analyze the structure of bulk sample material and it generates the two dimensional image of sample material of any

size and thickness. It can be used to generate high resolution images of sample material surface and can provide the information of about less than 1 nanometer (<1nm) in size.

The JEOL JSM-6480LV scanning electron microscope (SEM) was used to analyze the prepared TiO_2 sample and study the particle morphology and structure. The platinum material was used to coat the samples and then these coated samples were used for SEM analysis.

3.2.4. UV-VISIBLE SPECTROSCOPY

Most of the molecules absorb ultraviolet light or visible light. If there is reduction in strength of beam thus there is increase in absorption of light in solution. It is based on principle of Beer-Lambert law (at fixed path length) which states that the absorbance is directly proportional to the path length of light and the concentration of the sample solution. Different molecules absorb different wavelengths of light. A spectrum of absorption will represent number of absorption bands which is corresponds to various structural groups within the molecule. In this it is very essential to know the how absorbance of solution changes with the concentration of solution.

By using UV-Visible spectrophotometer (Shimadzu, UVSPECTROPHOTOMETER) integrated with a computer system (*JASCO, V-530, Samsung*), the supernatant dye solution was analyzed at characteristic wavelength λ_{max}= 520 nm for determining the calibration curve of safranin (O) dye and to obtain the concentration of dye after degradation.

3.2.5. BRUNAUER-EMMETT-TELLER (BET)

Brunauer-Emmett-Teller theory was introduced by Stephen Brunauer, Paul Emmett and Edward Teller. BET uses the principal of physical adsorption of molecules of gas on the surface of solid to measure the specific surface area of sample material. BET mostly uses the non-corrosive gases (like Carbon dioxide, Nitrogen etc) as an adsorbate to determine the specific surface area. The BET theory concept is based on Langmuir theory which given for the monolayer adsorption of molecules. BET theory uses this theory for multilayer adsorption of molecule with the some postulates such as, molecules adsorbed on solid surface by physical adsorption, no interaction appears in between any adsorption layer and to each layer the Langmuir theory can be applied.

In this work, to measure the specific surface area of synthesized TiO_2 nanoparticles we used BET instrument manufactured by ‘Quantachrome Instruments’. The TiO_2 nanoparticles

calcinated at different temperature were degassed at 110 C for 2 hr before the study of adsorption and desorption of samples with liquid nitrogen to determine the specific surface area.

3.3. EXPERIMENTAL SETUP

A three neck 250mL conical flask having two connections off size 24/29 and one connection for thermometer inlet, one coneection off size 24/29 was equipped with pressure equalizing funnel for dropwise addition of hydrolysis solution i.e milliQ water into precursor solution present in conical flask.

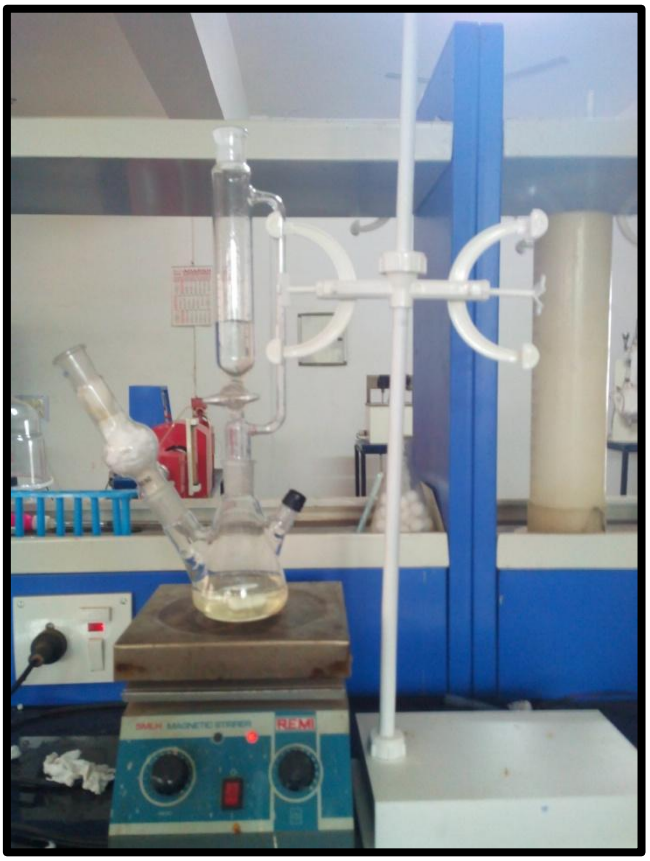

Figure 5 Setup for TiO_2 synthesis

A $CaCl_2$ drying tube is connected to conical flask through other connection of size 24/29. The drying tube is a simple tube filled with $CaCl_2$ desiccant substance, having one side open and other side having connection of size 24/29. It is used for releasing the pressure from flask while prohibiting moisture to be entered. Because reactions which are evolving gases or being heated could potentially shatter a sealed vessel, although, it may not be preferable to allow air moisture to enter the vessel. A drying tube releases pressure inside the reaction

vessel by allowing gases to escape whereas preventing moisture from contaminating the reactants. Magnetic stirrer used for the stirring the gel at 55-60^{0}C for 2hr and then at ambient temperature for about 15 hrs.

To carry out the photocatalysis degradation reaction, we prepared a photocatalysis reactor which includes a wooden box (30cm× 30cm× 70cm) having aluminium foil stick to the inner wall of box to provide reflection of light and hence provide maximum number of photons to the catalyst. This box connected with a high pressure mercury lamp (Bajaj, 125W) at top, used as a photon energy source. Magnetic stirrer placed inside the wooden box to supply stirring action to the reaction medium.

Figure 6 Setup for photocatalysis

3.4. EXPERIMENTAL PROCEDURE FOR TiO_2 SYNTHESIS

It is published in the various literatures that the synthesis of catalytically active TiO_2 nanoparticles with anatase phase from titanium tetra isopropoxide (TTIP) requires the addition of various hydrolyzing agents, like CH_3COOH–CH_3OH, aqueous HCl, H_2O_2, p-

toluene sulfonic acid, NH_4OH or HNO_3 and various additives such as urea, hexylene glycol, carbon, ZnO/Fe_2O_3, Al_2O_3, and ZnO_2. However, we have reported here a very simple sol– gel process to synthesize nanoparticles of TiO_2 from titanium tetra isopropoxide with absence of any additives or hydrolyzing agent.

Titanium tetra isopropoxide (25mL) and isopropyl alcohol (2-propanol) (75mL) were taken at ambient temperature in a 250mL conical flask connected with a pressure equalizing funnel, a thermometer inlet and a $CaCl_2$ guard tube. Temperature of this TTIP and isopropyl alcohol mixture (i.e. precursor solution) was increased to 60^o C. In this precursor solution which at 60^o C, a water (25.0mL) was slowly added (dropwise) for period of 30min at 55–60^o C. The thick whitish slurry was found after addition of water, this thick whitish slurry was stirred for 2.0 hr with a magnetic stirrer at the same temperature (60^o C); followed by stirring at ambient temperature for 15.0hr. Then filtration of the resulting material through Whatmann filter paper by vacuum filtration was carried. The cake that was obtained by filtration was washed by 25 mL of water, it is filtered and further obtained cake was washed by 25 ml of 2-propanol followed by filtration. The obtained doubled washed TiO_2 cake was dried in a hot air oven for about 12.0hr at 110^o C. This dried TiO_2 cake was crushed and squeezed to obtain powder and labeled as TiO_2-110.The dried TiO_2 powder was then calcined at 400, 600 and 800^o C for 2.0hr in a muffle furnace. These samples were labeled as TiO_2-400, TiO_2-600 and TiO_2-800.

3.5. PREPARTION OF STANDARD STOCK SOLUTION

100 mg of safranin (O) dye powder is accurately dissolved in 1000ml of distilled water. First of all, a 100 mg precisely weighted dye powder was allowed to dissolve in 200ml double distilled water by shaking thoroughly. After complete dissolution of dye it was transferred in a volumetric flask (1000ml) then double distilled water was added up to the 1 liter mark of volumetric flask. A stock solution prepared was 100 mg/liter (100 ppm) with double distilled water. By using this stock solution, next low concentration was prepared by subsequent dilution. The supernatant dye solution was analyzed at wavelength of 520 nm by using JEOL UV-Visible spectrophotometer.

Chapter 4

RESULTS AND DISCUSSION

4. RESULTS AND DISCUSSION

ABSTRACT: To study the photocatalytic behaviour of prepared TiO_2 nanoparticles, the information in the form of surface morphology, active surface area, crystal phase, purity (or presence of defects) and band gap energy is very important. These information we obtained by characterizing the synthesized TiO_2 nanoparticles using XRD, SEM, FTIR, BET and UV-vis spectroscopy analysis. The degradation of safranin (O) dye carried out by TiO_2 nanoparticles, optimization study was carried out by optimizing various parameters.

4.1. CHARACTERIZATION OF TiO_2 NANOPARTICLES

4.1.1. X-RAY DIFFRACTION (XRD) ANALYSIS

The XRD patterns of the prepared samples are presented in Figure 9.

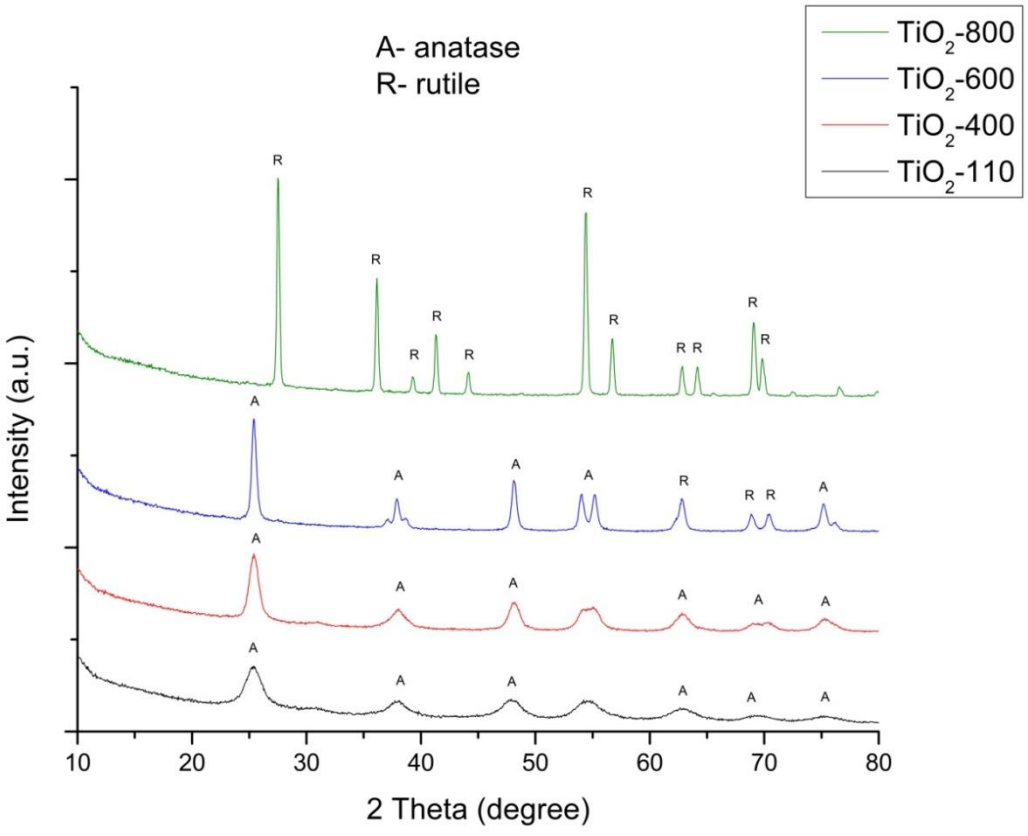

Figure 7 XRD analysis of TiO_2 nano particles calcinated at different temperature

The prepared TiO_2 nanparticles dried at 110^o C, and annealed at 400^o C (labelled as TiO_2-400) or 600^o C (labaled as TiO_2-600) shown well-specified diffraction peaks corresponding to anatase phase (JCPDS 21-1272), whereas TiO_2 powder calcined at 800^o C

(TiO_2-800) showed only rutile phase (JCPDS 21-1276). The size of the crystallites present in all samples rises with calcination temperature.

The average crystallite size of anatase phase and rutile phase were calculated by the commonly known Scherer equation using full width at half maximal (FWHM) data of each phase:

$$D = \frac{\kappa\lambda}{\beta \cos\theta}$$

Where, D is average crystallite size in angstrom unit (A^o)

K is shape factor and 0.9 is used.

λ is wavelength of incident x-ray radiation.

β is line width at half maximum intensity.

θ is Braggs angle

The average crystallite size of prepared TiO_2 samples ware calculated by using this equation were 9.4, 15.4, 18.8 and 54.12nm for TiO_2-110, TiO_2-400, TiO_2-600 and TiO_2-800 respectively.

4.1.2. FOURIER TRANSFORM INFRARED SPECTROSCOPY (FTIR) ANALYSIS

FTIR spectra of TiO_2 dried at 110^o C (TiO_2-110) and TiO_2 calcined at 400^o C (TiO_2-400), 600^o C (TiO_2-600) and 800^o C (TiO_2-800) are shown in Figure 10. The sharp peaks of TiO_2-400, TiO_2-600, TiO_2-800, at 2856 and 2926 cm^{-1} are assigned to the symmetric and asymmetric vibrations of –CH2- and –CH3 groups respectively. The band at about 1527 cm^{-1} and 1423 cm^{-1} corresponds to the C-O-H bending vibration, which is attributed to the presence of titanium isopropoxide. Bands less than 800 cm^{-1} are because of the Ti–O stretching vibration. A very broad band emerges in a range of 500~700 cm^{-1}, which is due to the vibration of Ti–O–Ti bonds in TiO_2 lattaice.

4.1.3. SCANNING ELECTRON MICROSCOPE (SEM) ANALYSIS

The surface morphologies of prepared nano size particles of TiO_2 are given in figure 11, The prepared nanoparticles have homogeneity in their shape. From figure we can say that, a tiny part of synthesized TiO_2 particles formed with an agglomeration of nanoparticles of TiO_2. It has clearly observed that TiO_2-800 sample (TiO_2 calcinated at 800^o C) has spherical

type structure and this type of structure isn't seen in TiO_2-110, TiO_2-400 and TiO_2-600 sample. Because TiO_2-800 sample (contains rutile form only) has better crystallinity than other sample (which consist either anatase phase or anatase and rutile mix phase)

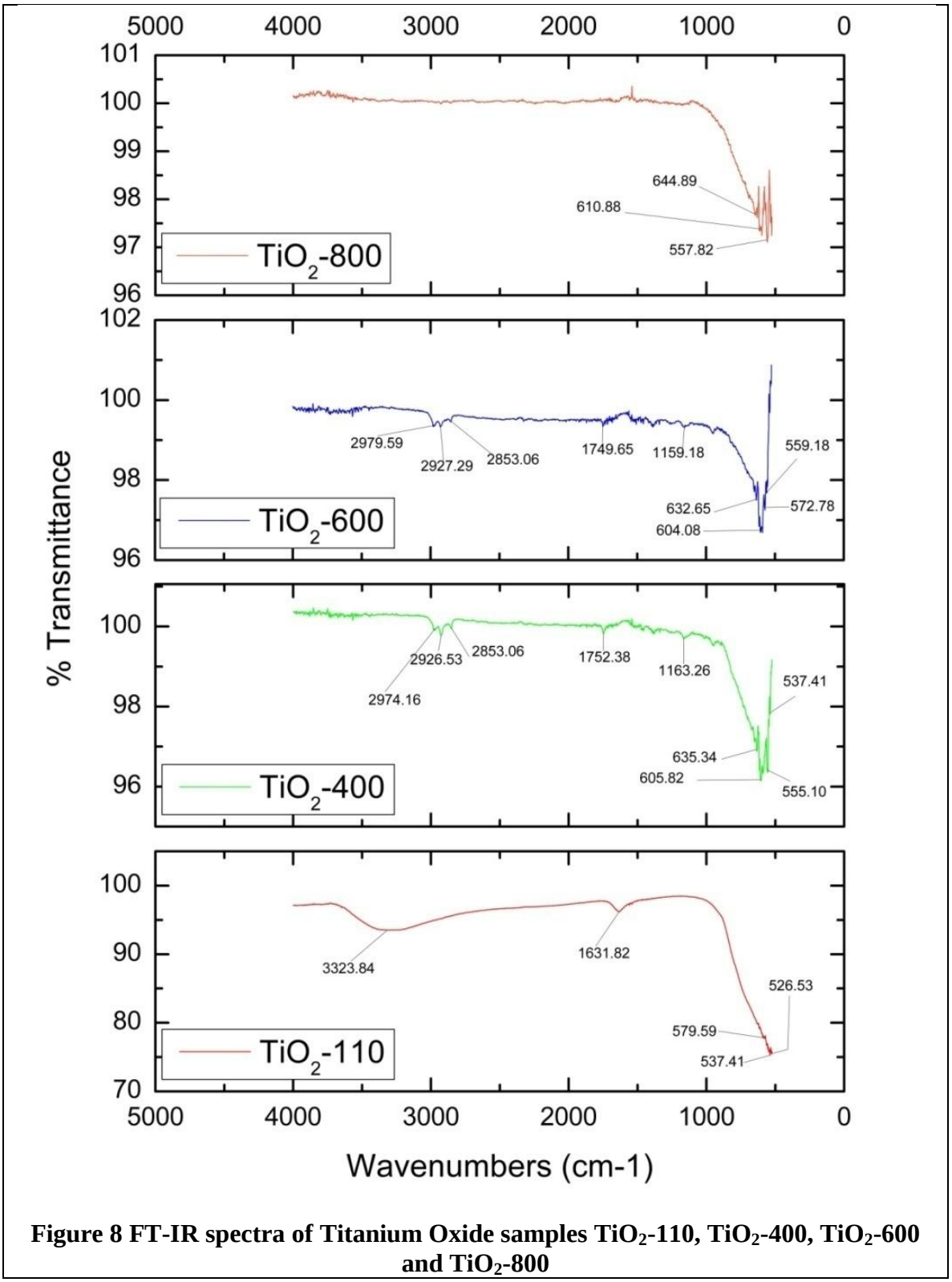

Figure 8 FT-IR spectra of Titanium Oxide samples TiO_2-110, TiO_2-400, TiO_2-600 and TiO_2-800

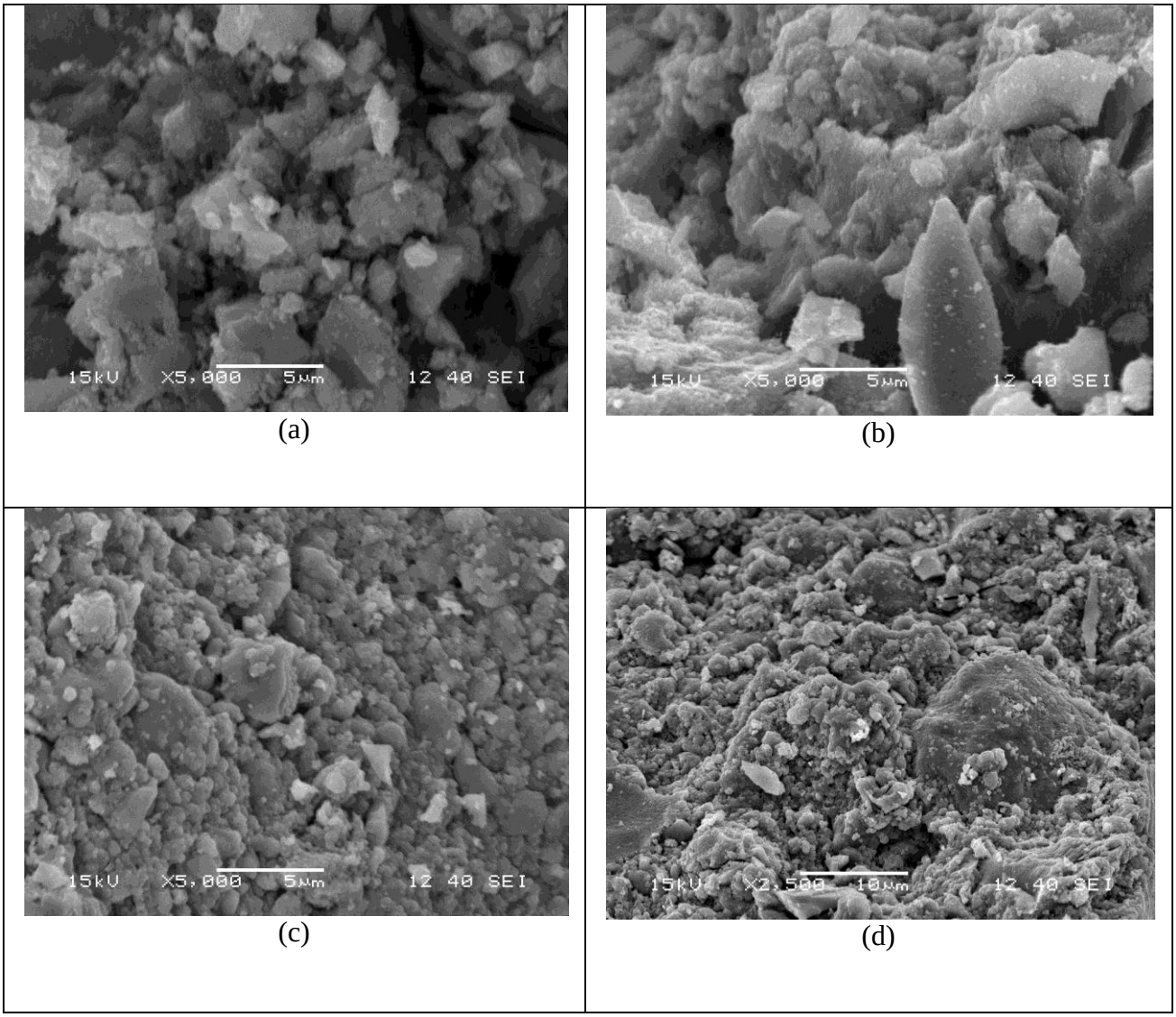

Figure 9 SEM images of (a) TiO_2-110 (b) TiO_2-400 (c) TiO_2-600 (d) TiO_2-800

4.1.4. ULTRAVIOLET-VISIBLE SPECTROSCOPY ANALYSIS

UV-visible diffuse reflectance spectra of nanoparticles of TiO_2 are given in figure 11. From this spectra we can conclude that, slightly increase in the absorption of TiO_2 samples calcinated at different temperatures than TiO_2-110 sample in over a wide range of visible light but in UV light region TiO_2-600 and TiO_2-800 shows decreased in their absorption compared to TiO_2-110 sample. The TiO_2 calcinated at 400^o C (TiO_2-400) has shown tremendous absorption, nearly three times than that of TiO_2-110 sample in UV light region. For higher photocatalytic activity, TiO_2-400 sample can be employed because it excites to produce more electron-hole pairs under visible light as well as UV light. The Band gap (E_g) energies of TiO_2-110, TiO_2-400, TiO_2-600 and TiO_2-800 were 3.45, 3.7, 2.8 and 2.85 respectively. These band gap energies determined by plotting the graph between (αhv)^2 on

y-axis and hv on x-axis (allowed direct transitions). Where α is absorbance calculated from UV and hv is photon energy (calculated by hv= 1280/wavelength)

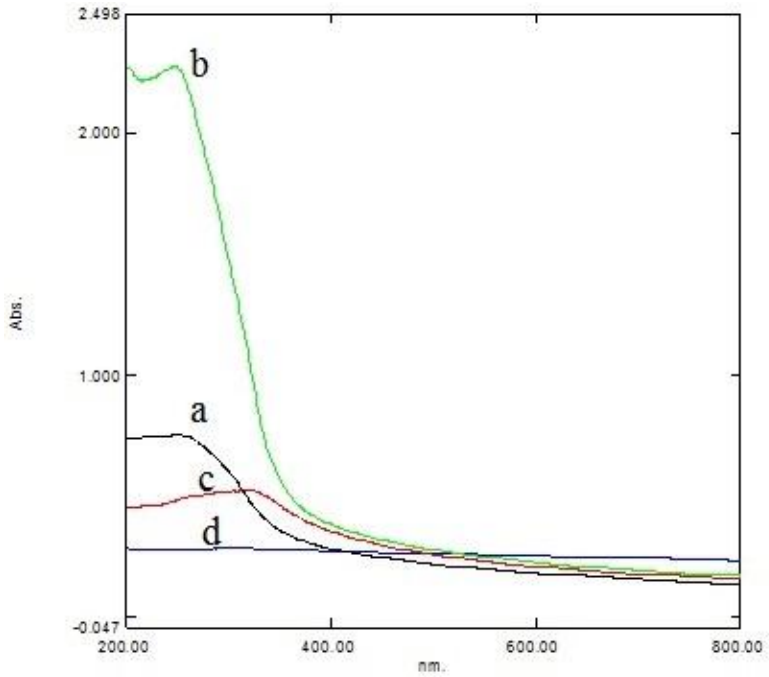

Figure 10 UV-Visible spectra of (a) TiO_2-110, (b) TiO_2-400, (c) TiO_2-600 and (d) TiO_2-800

4.1.5. BRUNAUER-EMMETT-TELLER (BET) ANALYSIS

The surface area of prepared TiO_2 material calcinated at different temperature was evaluated by BET- nitrogen adsorption technique are shown in table 4,

Table 4 Specific surface area of TiO_2 samples by BET theory

Samples	***Specific surface area (m^2/g)***	***Average particle size calculated by XRD (in nm)***
TiO_2-110	*101.318*	*9.4*
TiO_2-400	*95.448*	*15.4*
TiO_2-600	*48.881*	*18.8*
TiO_2-800	*43.635*	*54.1*

From above table we have noticed that, anatase phase (i.e. TiO_2-400) have higher specific surface area, on comparison with rutile phase (i.e. TiO_2-800). Also it shows as clacination temperature increases the specific surface area of prepared TiO_2 nanoparticles

increases, due to increases in particle size when temperature changes from 110 to 800^{o} C and change of phase occurred.

4.2. STUDY OF PHOTOCATALYTIC DEGRADATION

The photo-degradation of Safranin (O) dye was studied in a simple photo-reactor (described before in section 3.2 & shown in figure 8) which is fabricated as a part of research project. The photocatalytic study of prepared TiO_2 nanoparticles was done by degradation of Safranin (O) dye under the irradiation of light. A 50 mg of synthesized TiO_2-110 sample was taken in a 250 ml beaker containing 200 ml of safranin (O) dye solution having concentration 5 ppm. This solution was then kept inside the chamber of photo-reactor with light ON and stirring was started (~400 rpm). With every 20 minutes 3ml of sample was pipette out till the color changes to colorless. The taken samples ware then analyzed in the *JEOL UV-Visible Spectrophotometer* to determine the absorption spectrum. Same procedure was used for other synthesized TiO_2-400, TiO_2-600 and TiO_2-800 samples.

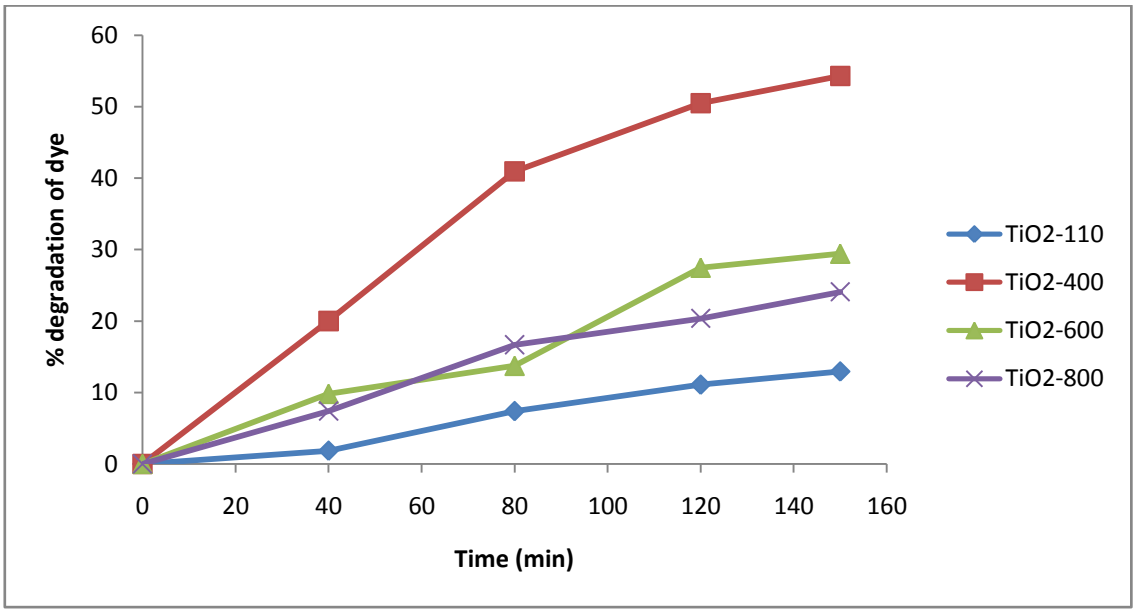

Figure 11 Photo-degradation of safranin (O) dye on the prepared TiO_2 samples

From above graph we can conclude that, TiO_2-400 sample shows the highest photocatalytic degradation of safranin (O) dye (about 55% in 150 min). So it's quite clear that, TiO_2 calcinated at 400^{o} C (anatase phase) has great potential to degrade safranin (O) dye. Therefore for further optimization of parameters of photocatalysis process we used only TiO_2-400 sample.

4.2.1. CALIBRATION CURVE

A calibration is a common method of obtaining the concentration of a substance in an unknown solution, by comparing it with, the concentration of substance in a known solution having set of standard solutions. It is also known as analytic signal because of the plotting of calibration curve according to the response of instrument and this response varies with measured substance (analyte) concentration. In calibration curve, a series of standards was prepared across the range of concentration close to the concentrations of unknown analyte. The concentrations of the prepared standards must reside under the working range of the instrument. For most substances a plot between response of instrument (absorbance in UV analysis) and concentration of analyte shows a linear relationship. However, the non-linearity in calibration curve can be avoided by diluting the analyte into the linear range or compensated by using non-linear curve fitting methods.

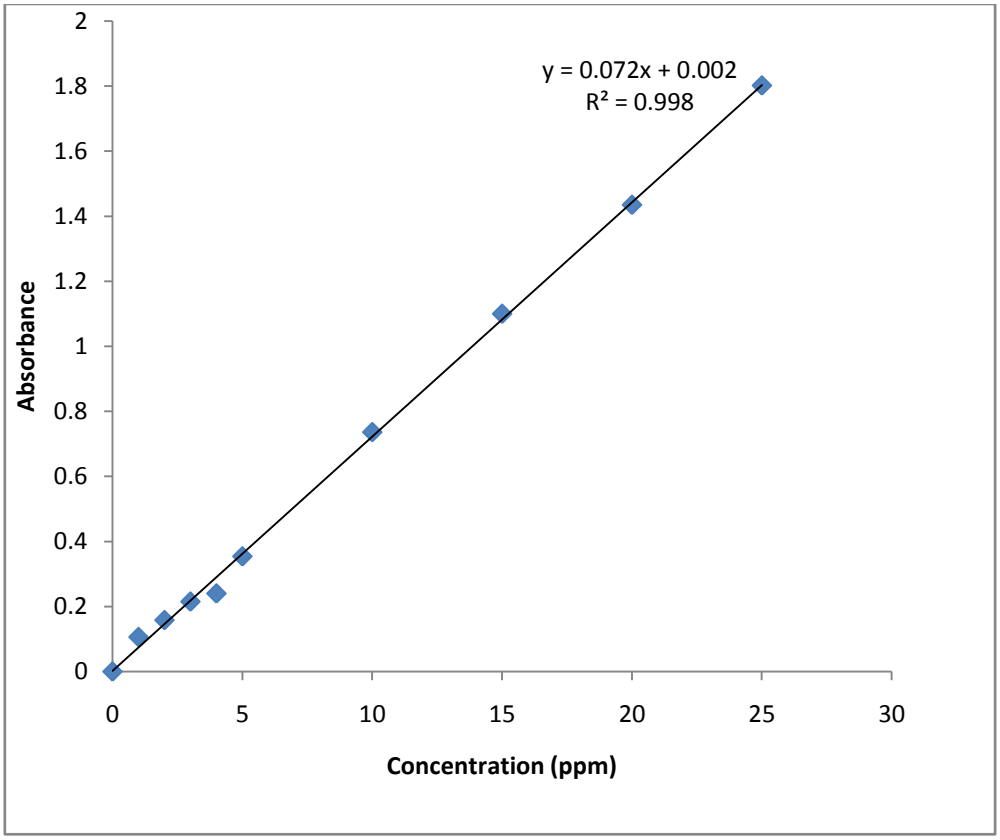

Figure 12 Calibration curve of Safranin (O) dye, λ_{max}=520 nm.

We can measure the response of unknown analyte by using instrument and by interpolating this response we can determine the concentration of unknown analyte. A main

advantage of calibration curve method is random errors in preparing and analyzing the standard analyte solutions were averaged over several standards.

4.2.2. OPTIMIZATION OF VARIABLES IN PHOTODEGRADATION

In this we studied, effect of various operational variables such as effect of catalyst dose, initial concentration, pH and temperature on the photo-degradation of safranin (O) dye by using synthesized heterogeneous TiO_2 photocatalyst.

4.2.2.1. EFFECT OF CATALYST DOSE

In photocatalytic degradation studies catalyst dose plays an important role because of cost of photocatalyst used and for an effective degradation of safranin (O) dye. If we use less amount of catalyst then the rate of degradation will decrease, however, if we use large amount of catalyst then it will cost more for degrading the given dye. Hence obtaining the optimum dose is always cost effective for maximum degradation with minimal resource. So there is a great importance for study the effect of catalyst dose on photocatalytic degradation.

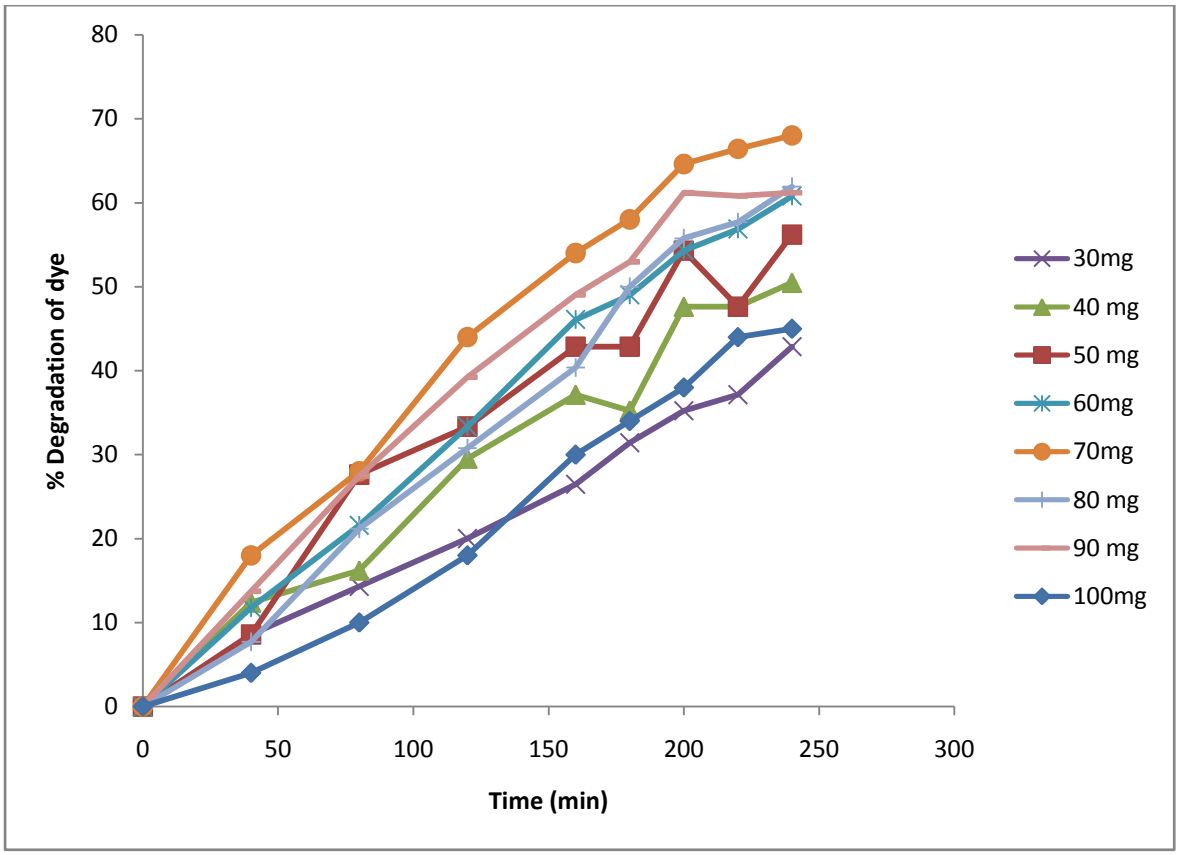

Figure 13 Graphical representation of effect of catalyst dose

To study the effect of catalyst dosage, different dosages of TiO_2 photocatalyst as varies from 30 mg (0.03g) to 100 mg (0.1g) were taken into 250 ml beaker which contain 200 ml safrinin (O) dye having concentration 5 ppm (5 mg/l) and pH= 7.78 (measured when we made the 5 ppm dilution). This sample was kept in photo-reactor for a period of 240 minutes, with mercury lamp switched ON and sample was stirred by magnetic stirrer (400 rpm) while doing experiment. A plot of % degradation of safranin (O) dye for various catalyst doses versus time was plotted figure 12,

From above figure it was found that with increase in TiO_2 photocatalyst dosage, percentage (%) degradation of Safranin (O) was increased and it reaches to an optimum value of catalyst dose (70 mg) at which the % degradation of dye was maximum (73% degradation) for the period of 240 mins. After that optimum catalyst dose % degradation was decreased. These results can be described by, in terms of availability of large number of active sites on the catalyst surface and penetration of light into the sample suspension. As catalyst dose increases the number of active surface area of TiO_2 nanoparticles were increases, but on the other hand it increases the turbidity of the safranin (O) solution so the penetration of light into the safranin (O) solution will decreases as a result of increased effect of scattering. The optimum dose of catalyst for photo-degradation of safranin (O) dye was found to be 14 mg/200 ml (70 mg/lit).

4.2.2.2. EFFECT OF INITIAL CONCENTRATION

To investigate the effect of initial concentration on photo-degradation process, the different concentrations of safranin (O) dye were used. The experiments were carried out with fixed TiO_2 photocatalyst dose of 70 mg/lit at varying initial concentration of safranin (O) dye as 5, 10, 15, 20 and 25 ppm (mg/lit) prepared from stock solution of 100 ppm.

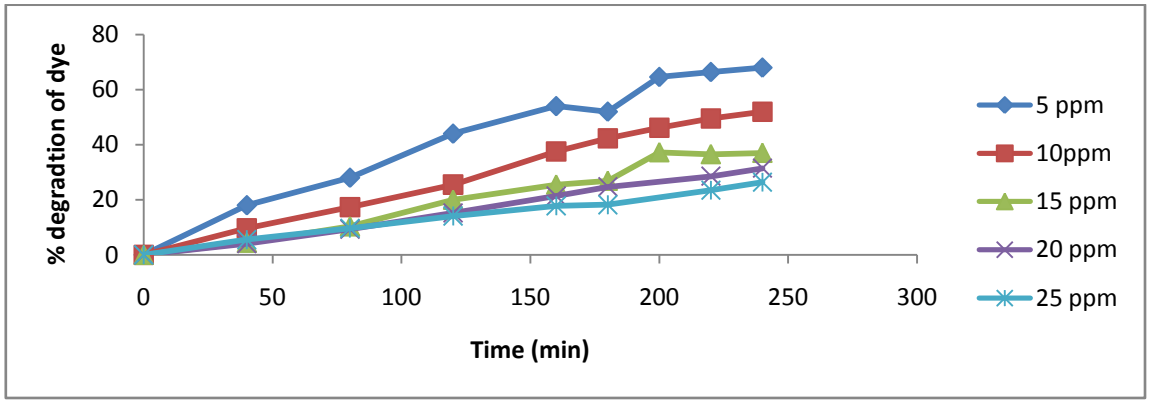

Figure 14 Graphical representation of effect of initial concentration

Obtained data were plotted as the % degradation versus time and the results obtained are shown in figure 13. From this plot we can conclude that, the percentage degradation of safranin (O) dye decreases as initial concentration of dye increases. Reason behind this is, as concentration of safranin (O) dye increases, more amounts of reactant(s) and reaction intermediate(s) are adsorbed on the surface of TiO_2 photocatalyst and it forms the layer on the surface, hence it will reduce the formation of hydroxyl radicals. This is because; the less number of active sites available for adsorption of water molecule for formation of hydroxyl ion as well as increase in turbidity (due to increase in initial dye concentration) will block the photon to activate the photocatalyst. The highest % degradation obtained at 5 ppm initial concentration and hence it was taken as optimum initial concentration of dye.

4.2.2.3. EFFECT OF pH

One of the most important factors which control the photo-degradation process is pH effect. The effect of pH on photocatalytic degradation of safranin (O) dye was studied in the pH ranging from 4 to 12 with 200ml of 5 ppm of initial concentration of safranin (O) dye and a dose of 70 mg/lit of TiO_2 photocatalyst. The pH of safranin (O) solution was adjusted by using the 0.1M HCl and 0.1M NaOH before the experiments. Also the pH of safarnin (O) saolution was measured before and after the process of photocatalytic degradation for determining the difference in pH.

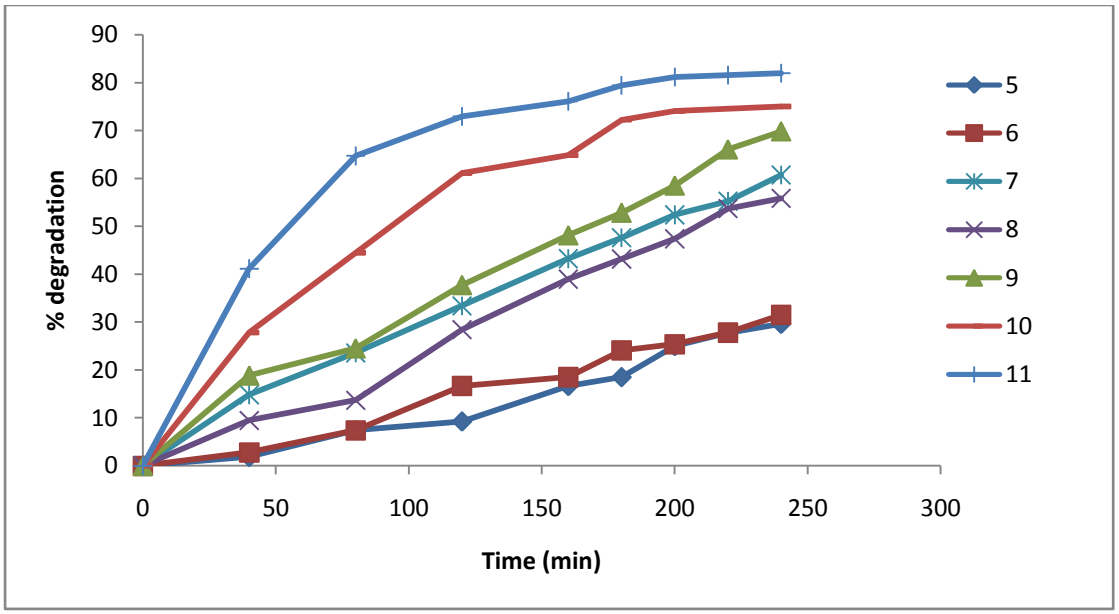

Figure 15 Graphical representation of effect of pH

As pH increases the degradation of safranin (O) dye also increases. At acidic pH range the degradation efficiency of safranin (O) dye was less, because of dissolution of TiO_2

nanoparticles at low pH [41]. While at basic pH range the photo-degradation found to be increased due to the pH influenced the surface properties of photocatalyst as well as it influenced the dissociation of the dye and formation of OH radical in the solution.The main reason behind the increase in photo-degradation process is formation of hydroxyl ion is higher at higher pH. The optimum pH was obtained, pH=11, at which % degradation was maximum.

4.2.2.4. EFFECT OF TEMPERATURE

In this study we also investigated the effect of temperature on photocatalytic degradation process of safranin (O) catalysed by TiO_2 photocatalyst with varying the temperature in the range from 40 to 70 C at interval of 10 C. Also the study was carried out with 70 mg/lit of catalyst in a dye solution having initial concentration of 5 ppm exposed to light for a 240 minutes.

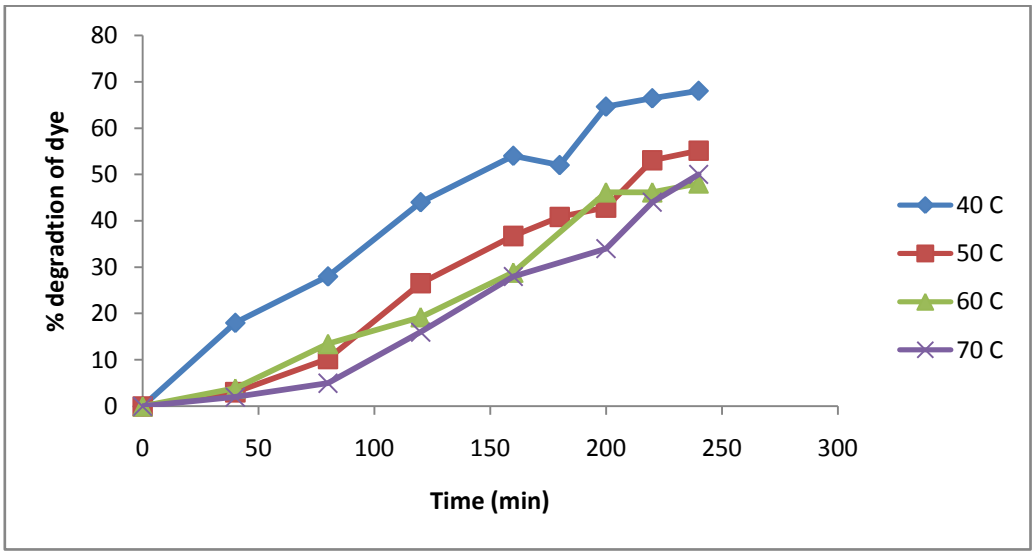

Figure 16 Graphical representation of effect of temperature

It can be seen in figure 18, that the photocatalytic degradation of safranin (O) dye decreases as temperature of dye solution increases, but, in most of the cases the higher the temperature faster the degradation rate. The results from figure 18 can be explained as; the rise in temperature of dye solution lowers the absorbability of TiO_2 photocatalyst to safranin (O) dye. The lower absorbability of Safranin (O) will weaken the direct hole oxidation on TiO_2 photocatalyst surface. The maximum degradation of dye occurs at a temperature of 40 C and taken as a optimum temperature at which rate of degradation was maximum.

4.2.3. KINETICS OF PHOTOCATALITIC DEGRADATION

The photocatalytic degradation of safranin (O) organic pollutant on the TiO_2 nanoparticles surface follows the kinetics of pseudo first order and can be expressed as,

$$-\ln (C_s/C_{s0}) = kt$$

Where, C_s = concentration of safranin (O) dye (in ppm) after a time t in (mins),

C_{s0} = concentration of safranin (O) dye (in ppm) at time t=0 min,

k = the pseudo fiest order rate constant of photo-degradation process,

t = time in mins.

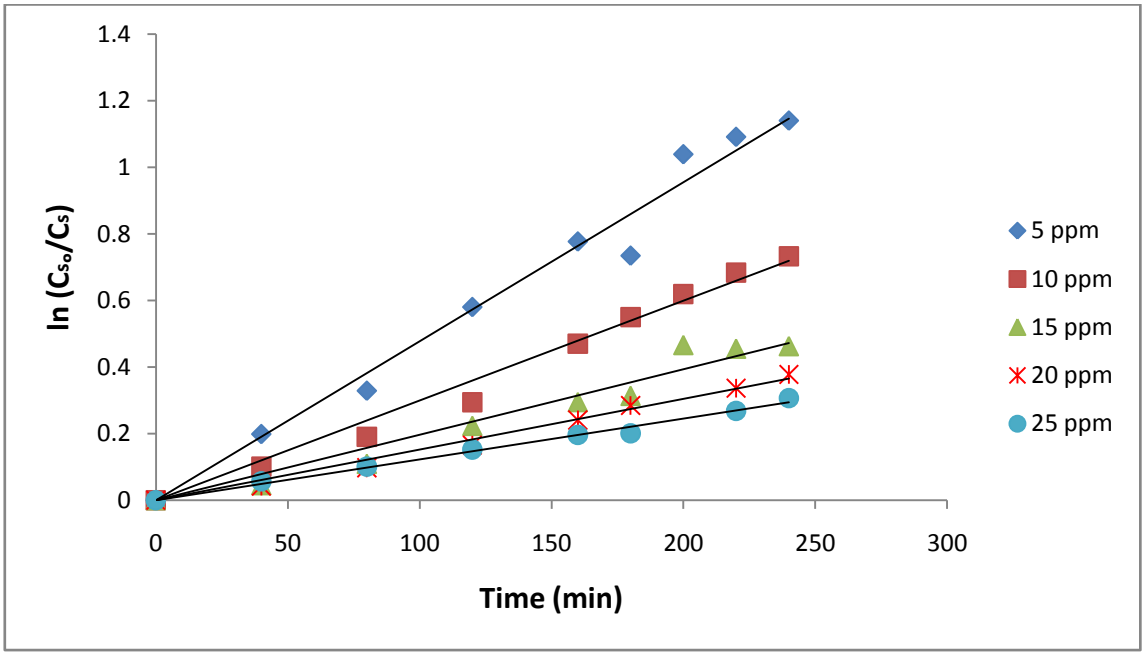

Figure 17 Kinetics of Photocatalytic degradation by varying initial concentration

A plot of $\ln(C_{s0}/C_s)$ versus irradiation time (t) is shown in figure 14 for safranin (O) dye degradation. It is quite clear that there exist a linear relation between $\ln(C_{s0}/C_s)$ and time. The pseudo first order rate constant for photo-degradation process k and R, linear regression coefficient with various safranin (O) dye concentration are given in table 5. From table, the least square fit, R^2 = 0.9795 and rate constant of degradation 0.0048 min^{-1} was evaluated as evaluated. The linear relationship between the functions with large R^2 values was observed. Increase in initial concentration of dye from 5 ppm to 25 ppm decreases the rate constant from 0.0048 to 0.0012 min^{-1}in 240 minutes. There was decrease in photo-degradation rate constant as increase in initial concentration of safranin (O) dye solution can be described as, the initial concentration of safranin (O) solution increases the path length of photons which

are penetrating the solution decrease. While reverse effect was observed in low initial concentration of dye.

Table 5 Rate constants of photo-degradation process with different initial concentration

Experiments	***TiO_2 concentration (mg/lit)***	***Initial concentration of safranin (O) dye solution (mg/lit)***	***Rate constant of degradation, k (min^{-1})***	***R^2***
1	*70*	*5*	*0.004776*	*0.9795*
2	*70*	*10*	*0.002998*	*0.9851*
3	*70*	*15*	*0.001966*	*0.9562*
4	*70*	*20*	*0.001521*	*0.9887*
5	*70*	*25*	*0.001226*	*0.9916*

At high concentration, the molecules of safranin (O) dye may absorbed a notable amount of photons rather than the catalyst. Thus reduce the efficiency of catalyst at higher concentration of dye. Also this fact can be explained by Lingmuir-Hinshelwood model as firstly the organic safranin (O) dye adsorbed on the surface of man-sized TiO_2 particles and then the photocatalytic degradation takes place by irradiation with photon energy. Whereas, quenching between these excited safranin (O) molecules (which was irradiated by photon energy) will occur. The probability of quenching could also increases as initial concentration of safranin (O) dye increases. Consequently, the efficiency of photocatalytic degradation of safranin (O) dye solution is decrease with the increase of initial concentrations of safranin (O) dye solution.

CONCLUSIONS

CONCLUSIONS

Over the past decades, the tremendous effort put into TiO_2 nanomaterials has resulted in a rich database for their synthesis, properties, modifications, and applications. In this project, we first summarized the structural features of the four TiO_2 polymorphs that have been commonly seen in TiO_2 nanostructures. Also we report here a simple method of sol–gel process to obtain nanoparticles of anatase phase as well as rutile phase TiO_2 from titanium (IV) isopropoxide without using any hydrolyzing agent or additives. The advantage of sol-gel method are ambient temperature sol preparation and gel processing, high purity of precursors, product homogeneity, and good control on powder particle size and shape. The combustion of gel powders, crystallization of the amorphous TiO_2 and phase transitions of different phases are discussed. The photocatalytic activity of prepared various TiO_2 sample was studied on degradation of safranin (O) dye. It was found that TiO_2-400 (anatase phase) shows tremendous photocatalytic activity on safranin (O) dye degradation. This photocatalytic degradation of safranin (O) was optimized to obtained higher degradation rate. Experiment results shows that the maximum photocatalytic degradation was obtained at pH=11. The optimum parameter we determined were, 70 mg/lit of catalyst dose, 5 ppm initial concentration and 40 C temperature.

FUTURE SCOPE

The following recommendation to be done for further studies:

- The photocatalytic studies using various electron scavengers like H_2O_2, $KClO_3$, $KBrO_3$, KIO_4 and $K_2S_2O_8$ on decomposition of Safranin (O) dye.
- The photocatalytic studies using electron scavenger and TiO2 photocatalyst on safranin (O) dye.
- The synthesis and coating of TiO_2 with different materials and its photocatalytic study.

REFERENCES

REFERENCES

1. M Anbia., S. A. Hariri, S. N. Ashrafizadeh, Adsorptive removal of anioic dyes modified nanoporous silica SBA-3, *Appl. Surf. Sci.*, 256 (2010) 3228–3233.
2. A.W.M. Ip, J.P. Barford, G. McKay, Reactive Black dye Adsorption/Desorption onto Different Adsorbents: Effect of Salt, Surface Chemistry, Pore Size and Surface Area, *J. Colloid Interface Sci*., 337 (2009) 32–38.
3. M. K. Purkait, S. D. Gupta, S. De, Adsorption of eosin dye on activated carbon and its surfactant based desorption, *J. Environ. Management,* 76 (2005) 135–142.
4. K. M. Shah, Handbook of Synthetic Dyes and Pigments, 2nd ed., Multitech Publishing Co., India, 1998.
5. L. Rejniak, H. Piotrowska,Effect of Malachite Green, Congo Red and Safranin on Cell Division in Gemmae of *Allium cepa*,*Nature*, 209 (1966) 517–518.
6. P. Chowdhury, T. Viraraghavan, Sonochemical degradation of chlorinated organic compounds, phenolic compounds and organic dyes – A review, *Sci. Total Environ*, 407 (2009) 2474–2492.
7. E. Forgacs, T. Cserhati, G. Oros, Removal of synthetic dyes from wastewaters: A review, *Environment International*, 30 (2004) 953–971.
8. V. K. Gupta, I. Ali, T. A. Saleh, A. Nayak, S. Agarwal, Chemical treatment technologies for waste-water recycling—an overview, *RSC Advances*, 2 (2012) 6380–6388.
9. W. Z. Tang, H. An, UV/TiO_2 photocatalytic oxidation of commercial dyes in aqueous solutions, *Chemosphere*, 31 (1995) 4157-4170.
10. V. K. Garg, R. Gupta, A. B. Yadav, R. Kumar, Dye removal from aqueous solution by adsorption on treated sawdust, *Bioresource Technology*, 89 (2003) 121–124.
11. A. K. Golder, N. Hridaya, A. N. Samanta, S. Ray, Electrocoagulation of methylene blue and eosin yellowish using mild steel electrodes, *J. Hazard. Mater.*, 127 (2005) 134–140.
12. N. K. Lazaridis, T. D. Darapantsios, D. Georgantas, Kinetic analysis for the removal of a reactive dye from aqueous solution onto hydrotalcite by adsorption, *Water Res.*, 37 (2003) 3023–3033.
13. C. R. T. Tarley, M. A. Z. Arruda, Biosorption of heavy metals using rice milling byproducts: characterisation and application for removal of metals from aqueous effluents, *Chemosphere*, 54 (2004) 987–995.

14. M. R. Hoffman, S. T. Martin, W. Choi, D. W. Bahnemann, Environmental applications of semiconductor photocatalysis, *Chem. Rev.*, 95 (1995) 69–96.
15. N. Sobana, M. Muruganadham, M. Swaminathan, Nano-Ag particles doped TiO_2 for efficient photodegradation of direct azo dyes, *J. Mol. Catal.*, A 258 (2006) 124-132.
16. R. Zallen, M. P. Moret, The optical absorption edge of brookite TiO_2, *Solid State Commun*., 2006, 137, 154.
17. G. Wakefield, M. Green, S. Lipscomb, B. Flutter, Modified titania nanomaterials for sunscreen applications - reducing free radical generation and DNA damage, *Mater. Sci.Technol.*, 20 (2004) 985-988.
18. B. Liu, E. S. Aydil, Growth of Oriented Single-Crystalline Rutile TiO_2 Nanorods on Transparent Conducting Substrates for Dye-Sensitized Solar Cells, *J. Am. Chem. Soc.*, 131 (2009) 3985-3990.
19. A. Fujishima, K. Honda, Electrochemical photolysis of water at a semiconductor electrode, *Nature*, 238 (1972) 37-39.
20. X. Chen, S. S. Mao, Synthesis of titanium dioxide (TiO2) nanomaterials., *J. Nanosci. Nanotechnol.*, 6 (2006) 906-925.
21. E. Roduner, Size matters: why nanomaterials are different, *Chem. Soc. Rev.*, 35 (2006) 583-592.
22. Y. F. Chen, C. Y. Lee, M. Y. Yen, H. T. Chiu, The Effect of Calcination Temperature on the Crystallinity of TiO2 Nanopowder," Journal of Crystal Growth, *J.Crystal Growth*, 247 (2003) 363-370.
23. J. F. Banfield, D. R. Veblen, Conversion of Perovskite to Anatase and TiO2 (B): A TEM Study and the Use of Fundamental Building-Blocks for Understanding Relationship among the TiO2 Minerals, *Am. Mineral.*, 77 (1992) 545-557.
24. X.-Q. Gong, A. Selloni, M. Batzill, U. Diebold, Steps on TiO2 Anatase (101), *Nat. Mater.*, 5 (2006) 665-670.
25. O. Carp, C. L. Huisman, A. Reller, Photoinduced reactivity of titanium dioxide, *Progress in Solid State Chemistry*, 32 (2004) 33-177.
26. L. L. Hench, J. K. West, The sol-gel process, *Chem.Rev*, 90 (1990) 33-72.
27. C. J. Brinker , G. W. Scherer, Sol-gel Science: The Physics and Chemistry of Sol-gel Processing, *book*, Volume 3, Issue 10, October 199, page 522.

28. T C Jagadale, S P Takale, R S Sonawane, N-doped TiO_2 nanoparticle based visible light photocatalyst by modified peroxide sol-gel method, *J Phys Chem C.*, 112 (2008) 14595–14602.
29. J. H. Lee, Y. S. Yang, Effect of hydrolysis conditions on morphology and phase content in the crystalline TiO2 nanoparticles synthesized from aqueous TiCl4 solution by precipitation, *Mater. Chem. Phys.*, 93(2005) 237-242.
30. H. Zhang, J. F. Banfield, Kinetics of crystallization and crystal growth of nanocrystalline anatase in nanometer-sized amorphous titania, *Chem. Mater.*, 14 (2002) 4145-4154.
31. G. Oskam, A. Nellore, R. L. Penn, P. C. Searson, The growth kinetics of TiO2 nanoparticles from titanium(IV) alkoxide at high water/titanium ratios, *J. Phys. Chem. B*, 107 (2003) 1734-1738.
32. M. A. Behnajady, H. Eskandarloo, N. Modirshahla, M. Shokri, Investigation of the effect of sol–gel synthesis variables on structural and photocatalytic properties of TiO 2 nanoparticles, *Desalination*, 278 (2011) 10-17.
33. C. Burda, X. Chen, R. Narayanan, M. A. El-Sayed, Chemistry and Properties of Nanocrystals of Different Shapes, *Chem. Rev.*, 105 (2005) 1025-1102.
34. H. Tumma, N. Nagaraju, K. V. Reddy, Titanium (IV) oxide; an efficient and structure-sensitive heterogeneous catalyst for the preparation of azoxybenzenes in the presence of hydrogen peroxide, *Applied Catalysis A:General*, 353 (2009) 54–60.
35. V. Loryuenyong, K. Angamnuaysiri,J. Sukcharoenpong, A. Suwannasri, Sol–gel derived mesoporous titania nanoparticles: Effects of calcination temperature and alcoholic solvent on the photocatalytic behavior, *Ceramics Inter.*, 38 (2012) 2233-2237.
36. J. M. Herrmann, Fundamentals and misconceptions in photocatalysis, *Journal of Photochemistry and Photobiology A: Chemistry*, 216 (2010) 85-93.
37. S. Parra, J. Olivero, C. Pulgarin, Relationships between physicochemical properties and photoreactivity of four biorecalcitrant phenylurea herbicides in aqueous TiO_2 suspension, *Appl Catal B: Environ*, 36 (2002) 75-85.
38. Y. Kubota, C. Niwa, T. Ohnuma, Y. Ohko, T. Tatsuma, and T. Mori, Protective effect of TiO_2 particles on UV light induced pyrimidine dimer formation, *J Photochem Photobiol A: Chem*, 141 (2001) 225-230.
39. S. Cong, Y. Xu, Explaining the High Photocatalytic Activity of a Mixed Phase

TiO_2: A Combined Effect of O_2 and Crystallinity, *J. Phys. Chem. C*, 115 (2011) 21161-21168.

40. Kurkin, E.N Vorontsov, E.N. Savinov, Study of TiO_2 deactivation during gaseous acetone photocatalytic oxidation, *J. Catal.*, 186 (1999) 318–324.
41. A. Mukharjee, A. M. Raichur, J. M. Modak, Dissolution studies on TiO_2 with organics, *Chemosphere*, 61 (2005) 585-588.